# The use of wavelet analysis and the mixture model to study phase-locking related to task-set reconfiguration

Harro Meijer, 0898570
Thomas Gladwin, 0944882
Datum: 27 – 8 - 2001
Begeleider: prof. dr. R. De Jong
2e begeleider: dr. ir. L. J. M. Mulder
Instelling: Rijksuniversiteit Groningen
Experimentele en Arbeidspsychologie
Periode: September, 2000 tot September, 2001

## Abstract

Wavelet analysis provides information on the time course of the phase and amplitude of oscillations in non-stationary signals. The results of wavelet analysis are equivalent to those of the faster method of complex demodulation. We combined this method with the mixture model to identify differences in the time course of synchrony between brain areas during task-set reconfiguration. The mixture model provides a trial-by-trial likelihood of intention activation (de Jong, 2000), that is, of subject-driven reconfiguration prior to stimulus presentation. This allows prepared and non-prepared conditions to be distinguished within the switch condition, identical in every way except for the odds of preparation. Preliminary results could not, due to equipment failures, be reliably interpreted, but did indicate that this combined approach may provide interesting results in the future.

1.

# 2. Introduction

The primary purpose of our internship was to implement the use of wavelet analyses to extract rhythm characteristics from EEG signals (section 1.2). Pilot tasks we used to test the method can be found in appendix A. These tasks were concerned with short-term visual memory and perceptual binding. Section 1.3 provides details of the application of the method to task switching, our secondary objective. In that section we explain how the mixture model (de Jong, 2000) can distinguish, on a trial-by-trial basis, whether subjects had or had not prepared to switch to a different task. We used wavelet analyses to determine physiological differences between these response-determined conditions. The following section provides theory that may help to interpret the kind of physiological effects detectable by wavelet analyses.

## 2.1. Synchrony and the brain

After the theory introduced in section 1.2.1, we will provide an exact definition of synchrony in the context of the measurement of brain activity at the scalp. For now, we define synchrony in the brain as a period of rhythmic activity in two or more neuronal groups of which the "downbeats" of the rhythm (that is, action potentials) have a consistent separation in time. Discussion of the role of synchrony in cognition requires some theory concerned with cell assemblies.

### *2.1.1. Cell assemblies*

Distributed populations of neurons may become more strongly connected through the modified Hebbian learning rule (Pulvermüller, 1999), which states that correlated neuronal activity results in heightened synaptic sensitivity. This allows distributed neuronal populations, e.g. in visual cortex (Roelfsema, 1996; see section 1.1.2), to be activated by a single object, functional specialization resulting in a distributed coding of the object's properties (Roelfsema, 1996). Distributed, co-activated populations are termed cell assemblies and have ecologically and theoretically attractive properties.

Cell assemblies aid survival in a complex and changing world, and hence have significance for reproduction and evolution, by the way they avoid the combinatorial explosion that would follow from a strict separation of specific functions and representations (Roelfsema, 1996). This explosion would cause an undesirable trade-

off between the ability to make detailed and varied distinctions and the number of neurons to be maintened. Distributed coding is still subject, in principle, to this trade-off, but greatly increases the level of detailed variation for a given number of neurons by using them more efficiently, as the same neuron can then be used in a large number of different representations. This method of coding also allows novel stimuli to be represented as new combinations of known stimuli, and new tasks as new combinations of known actions, making representation both flexible and consistent. Finally, similar stimuli and actions will be represented by similar populations, which implicitly builds the concept of similarity, and hence the functions of categorization and abstraction, into the structure of the brain.

Cell assemblies' utility for theory comes from their provision of a framework for understanding dynamics between brain areas (see below) and the interplay between seriality and parallellity in cognition (Simon, 1994; see section 1.5). For instance, the cell assembly is an inherently parallel structure, but the space for cell assemblies to exist concurrently may be limited, and hence cell assemblies may have to come into existence sequentially.

Nunez' (2000) local / global theory states that global characteristics of brain activity are produced by large-scale features such as brain size, but also by local neuronal interactions, which are themselves influenced by global processes. The cell assembly model may help integrate the results obtained from the different levels, such as those provided by Nunez' (2000) methods for the global level and by Engel, König and Singer (1991) concerning in vitro studies (Nunez 2000, reply 1.3). Cell assemblies can be defined recursively, in the sense that a population of local cell assemblies may form a cell assembly at a more global scale. The processes associated with cell assemblies discussed in sections 1.1.2 and 1.1.3 may be the cause of activity at both local and global scales, and the cause of their interactions.

For the idea of a cell assembly to be useful, the neuronal groups participating in a cell assembly must be distinct in some way: this allows the question of what, exactly, the cell assembly is assembled of to be answered. We define the distinctiveness of two neuronal groups as the condition that cell assemblies exist such that the one neuronal group is not part of the assembly if and only if the other neuronal group is also a

member. It seems to make sense to consider subsets of a neural population that are not split up in terms of cell assembly membership as a unit; the population of interest and the relevant assemblies depend on the experimental context. An illustration of a distinct neuronal group is given in section 1.1.3, at which point assembly membership will have been related to synchrony. Neuronal groups can of course also be distinguished on other, e.g. anatomical, grounds, but such distinctions may become cloudy when the assembly of interest consists of component parts that themselves are composed of possibly widespread and anatomically heterogeneous neuronal groups. Unfortunately, specific relationships between anatomical characteristics and cell assembly memberships are beyond the scope of this paper.

Though distinct neuronal groups may themselves be cell assemblies on a smaller scale, and so forth on smaller and smaller scales, groups relevant to this and similar studies will have to be of a certain size and have certain characteristics. Section 1.2.3.2 provides details of the limitations of the EEG measurements we used. The most important result of these limitations is that the distinct neuronal groups of which we can measure the activity are sections of cortex with sizes in the order of about 5 square centimeters (Nunez, 2000, reply 1.7). This is about the scale of gross neural anatomy, which is also the scale of much neuropsychological data. The neuronal groups that we will consider will thus be lobes with broad subdivisions, and have functions like location representation, auditory processing, etc.

### *2.1.2. Binding*

If simultaneously activated cell assemblies overlap and still differently influence and are differently influenced by the rest of the brain, some kind of transient grouping must be involved. The brain has somehow evolved to solve this problem of grouping together the correct neuronal groups, as illustrated by the way visual information processing works (Roelfsema, 1996). Amongst other dimensions of visual objects, location and identity are represented separately in the brain, the perceived object being represented as the cell assembly consisting of all the perceived dimensions. If two or more objects are perceived simultaneously, the attributes of the one object must be explicitly coded in such a way as to distinguish them from those of the other. This coding of distinction and belonging has been labelled binding.

*2.1.3. Synchrony and its functions*

Engel, König and Singer (1991) have demonstrated that cells in cat visual cortex responding to two superimposed lights bars, presented at the same location with different orientations, become segregated into distinct assemblies by synchrony. Note that, because the light bars occupied the same region in visual space, their representations in the cortex must have overlapped. Coding in synchrony allowed the two simultaneously active sets of cells to overlap in space and still be distinguishable, which is just the function attributed to binding.

Aside from supplying an extra dimension for neuronal coding, synchrony exploits the property of coincidence detection, which refers to the inverse relationship of neurons' firing threshold and synchronization of their inputs (Azouz & Gray, 2000). Once a

*Figure 1.1 Oscillating networks*

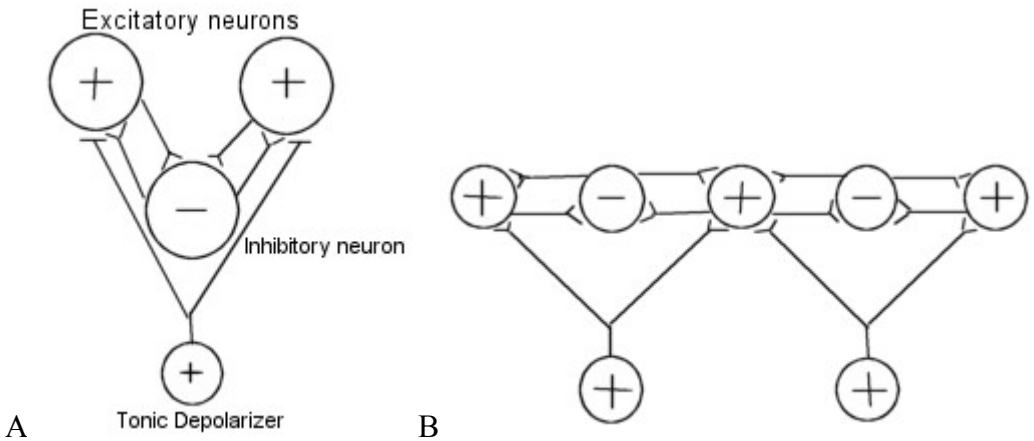


group of neurons with synchronous activity exists, coincidence detection could help to recruit large groups of neurons into an assembly (Azouz & Gray, 2000). How could such a pacemaker arise in the first place?

The most important cause of synchrony seems to be the structure of certain cortical networks (Sukov & Barth, 2001). Although specialized pyramidal pacemaker cells do exist (for instance, Gray & McCormick's (1996) chattering cells produce action potential bursts at frequencies between 20 and 70 Hz in response to depolarization) and may enhance synchrony or be preferentially tuned to certain frequencies (Sukov

& Barth, 2001), computer models (e.g. Traub et al., 1999) and in vitro studies (e.g. Buhl et al., 1998) have shown cortical pacemakers to be unnecessary for synchrony to occur. Sukov and Barth (2001) provide a pacemaker model in which the thalamus has a modulatory influence, which will be described after an example of a synchrony-causing network structure.

A simple network that oscillates in response to a constant excitatory input is given in figure 1.1 A (based on Eckhorn, 2000, in Miller (2000)). Activated excitatory neurons will produce post-synaptic potentials until their activity causes the central neuron to inhibit them, thereby shutting off its own excitation and allowing the process to begin again, and again, in a rhythm determined by properties such as the thresholds, strength of excitation and inhibition, etc.

Figure 1.1 B shows two overlapping networks, of which the middle neuron is distinct from its neighbors in the sense provided in section 1.1.1. This illustrates how synchrony can convey information on belonging; it disambiguates the situations where the marked neuron is bound to one or the other group.

Sukov and Barth (2001) propose a cortical circuit in which gamma frequency oscillations in the cortex are evoked by tonic depolarization caused by the thalamus. Two mechanisms produce synchronies in response to this depolarization. The first depends on excitatory and inhibitory reciprocal intralaminal interactions between pyramidal cells and inhibitory interneurons, which seems similar to the example from Eckhorn (2000) above. The second is based on interlaminal interactions, in which the supra- and intragranular layers reciprocally activate each other.

An interesting aspect of the Sukov and Barth model is that neural network processes involving the thalamus may have an effect on synchrony at the cortical level. Synchrony between possibly distant cortical locations mapped onto the thalamus might then be the output of neural circuitry that implements logical operators and is highly connected to other parts of the nervous system. This suggests that synchrony could occur at the cortical level in a wide variety of configurations, constrained, within biological parameters, by their learned usefulness for the organism at a given moment.

Coincidence detection suggests that synchrony not only provides the binding function, but also enhances the influence of representations that are part of cell assemblies. This could provide stability in cognition over short and long periods of time. At small time scales, the brain will not fluctuate between responses to varying sources of activity, but will respond primarily to coherent populations. Populations with heightened synaptic sensitivity due to experience will also be the ones most important in cognition in present situations, providing continuity over long periods.

The function of synchrony of most importance to this study is transient connectivity, which we distinguish from the transient grouping that occurs during, for example, perceptual binding. Consider a simple feedforward process in which tuned cells (Sukov & Barth, 2001; see above) respond selectively to members of a population oscillating at their preferred frequency, creating a grouping within the population. Note, however, that this grouping is a consequence of existing synaptic connections, only providing a connection in the sense that the conveyed information is grouped relative to receiving areas. Flexible cognition requires transient connections with an abstract synaptic function, for example mapping stimuli to responses. Since the brain has evolved to be sensitive to rhythmic qualities of neuronal activity, it seems reasonable to look to this coding dimension for an explanation of the flexibility in cognitive connections. Coincidence detection and pacemaker cells with preferred frequencies seem likely to play important parts in this function.

The following hypothetical model is intended to illustrate that synchrony could at least be part of a connective mechanism. A group of "fickle grandmother" pacemaker cells with different preferred frequencies and a wide range of connections could recruit oscillating cell assemblies representing actions or perceptions. Such a grandmother would have children, and children's children, but could swap them for other cell assemblies, at the time scale of change in oscillatory activity. Each member of a temporary family would receive coincident activation from the other members, providing feedforward and feedback loops, in which activation of one member activates the others. Grandmother cells may manipulate the inhibitor neuron in Eckhorn's model, perhaps competing amongst each other for the frequency of their potential family. The results presented in the next section provide some empirical

support for the association between synchrony and transient connectivity, although it should be clear that relationship between synchrony and transient connectivity is far from transparent. Even so, the combination of synchrony-causing network interactions and a transient connectivity function provide the possibility of a very powerful model for brain function.

### *2.1.4. Results concerning oscillations and synchrony*

Neuronal characteristics such as thresholds and synaptic strength and other biological parameters, such as propagation speed (Nunez, 2000) and the distance between synchronized cells (Nunez, 2000; Singer, 1993) together determine frequencies of oscillations and synchronies. We will not discuss the modeling literature that studies in detail the relative importance and interactions of these factors in causing oscillations of various frequencies; but see Kopell et al. (2000) for an example explaining different synchronization properties of beta and gamma oscillations based on synaptic strength and membrane conductance. The following results provide an overview of the situations in which oscillations of various frequencies occur, together with tentative interpretations and explanations based on theory presented so far.

#### *2.1.4.1. Delta / theta activity*

Harmony et al. (1996) predicted increases in delta activity (around 4 Hz) 1) during mental operations on a stimulus, 2) in response to increased difficulty, and 3) when irrelevant stimuli should be inhibited, and presented results supporting their prediction in the first two cases. They based their prediction on Vogel et al.'s (1968) distinction between classes I and II inhibition, which are both reflected in slow waves in the EEG. Class I inhibition occurs during slow-wave sleep and represents a global inhibition of excitatory processes. Class II inhibition is the task-related, selective suppression of irrelevant neural activity. Harmony et al. propose that attention to internal processing should be accompanied by class II inhibition, and hence increases in delta activity.

Nunez (2000) reports an increase in theta (4 – 7 Hz) coherence, especially between anterior and posterior regions, during mental calculations, relative to rest. Similarly, Sarnthein et al. (1998) found theta coherence between prefrontal and posterior association areas during working memory retention. Nunez (2000) notes that theta

coherence is low relative to alpha coherence, which is discussed below. He suggests that this may be a consequence of spatial resolution. As theta coherence is related to specific mental processes the underlying networks are likely to be smaller than the more global areas involved in alpha coherence.

One possible explanation of the association of delta / theta band activity with task-related inhibition is that delta activity reflects recruitment of assemblies at a frequency band that may be too slow to produce the benefits of coincidence detection. Even if depolarization is strong due to synchronous input, the cell membrane of a connected neuron may have time to return to its resting potential before the next pulse of inputs arrives, effectively dampening the effect of the output of the inhibited area and resulting in theta coherence between the inhibited and connected areas. At the same time, cells with characteristics allowing coincidence detection of slow oscillations may respond to the slower activity, allowing a coherent object to be the target of inhibition. If this hypothetical function of delta activity is the case, it would seem likely to play an essential part in negative priming (e.g. Tipper and Driver, 1988).

*2.1.4.2. Alpha activity*

An early finding concerning a relation between oscillations in the EEG and cognition was made by Berger (1929), who observed that performing mental operations such as arithmetic caused alpha rhythms, present in rest, to be replaced by irregular, fast oscillations. A general decrease in alpha coherence during mental calculations was found by Nunez (2000). This coherence decrease occurred at the same time as the increase in theta coherence mentioned above. Alpha amplitude was decreased most over posterior sites, but alpha coherence decreased most between frontal electrode pairs. This fits with the explanation provided later. Nunez noted that the precise frequency bands in which alpha coherence effects are strong might be narrow; choosing too broad a frequency band for analysis may thus obscure effects.

Klimesch et al. (1996) found a number of intriguing relations between memory performance and decreases in localized synchronization (event-related desynchronization, ERD; note that this measure is based on power at electrodes, not phase relations between them; see section 1.2.1) in the lower and upper alpha band (around 9 and 12 Hz respectively). They present an interpretation of different alpha

activity of good and bad performers based on the functional significance of the upper and lower alpha bands, desynchronization in these bands reflecting encoding (the upper band) and attention (the lower).

Two kinds of explanations arise for these results. Desynchronization suggests separation as opposed to grouping or connection. Separation of activity may be necessary to allow local processes to proceed without the disruption of new inputs arriving with the force of synchrony. However, it may also be the case that local processes do not require desynchronization, but cause it simply because local network interactions come to determine cell activity more than global alpha activity (see below). Whether separation is cause or effect, the consequent lack of coincidence detection may also serve a delay function, making sure even strong local activity remains localized. The memory model of Moscovitch (1992) discussed in section 1.1.5 proposes functional neuronal units of which the inner workings are unavailable to consciousness. Alpha desynchronization may be the method of keeping such black boxes closed.

The question remains why it is specifically alpha activity that seems to oppose the integrity of local processes. One possibility is that oscillations in the alpha band mostly reflect boundary conditions such as the size and shape of the brain and the propagation speed of electric waves traveling through it via synaptic activity (Nunez, 2000) and are therefore both strong and unrelated to specific local processes. Roughly reasonable estimates of propagation speed and brain size provide some support for a simple example of this interpretation. A wave traveling from one end of the brain to the other over the cortex (say 20 cm) at a speed of 5 m / s (a little lower than the 6 – 9 m / s estimate given by Katznelson (1981) and Nunez (1995)) would result in a "return-trip" taking 2 * 0.2 / 5 = .08 s, and an oscillation of 12.5 Hz. The different topography of amplitude and coherence decreases mentioned above seem logical given this explanation. Frontal areas seem likely to be involved in mental calculations, local processes dominating their own oscillatory activity. If alpha activity is indeed caused by wave-like effects over the brain, its amplitude at all areas seems likely to be attenuated if the interacting waves are disturbed by strong local processes. However, what is left of the alpha waves may still be coherent at regions other than the disturbing ones.

*2.1.4.3. Beta activity*

Pfurtscheller et al. (2000) found beta oscillations (14 - 32 Hz) in the EEG over somatosensory cortex during voluntary finger movements. The frequencies with the highest activities were location-specific, around 17 Hz over the hand area and 23 Hz over the foot area. Roelfsema et al. (1997) found beta synchronization between areas 7 and 51 in cat cortex during a task in which a lever had to be pressed in response to a change in grating orientation.

The dependence on structural properties of underlying tissue suggested by beta activity's location-specificity suggests that this kind of activity primarily reflects the activation of specialized neural networks. The synchrony occurring after associative learning fits well with this interpretation because of the presumable formation of a new cell assembly during training. Given the same approximations as were used for alpha activity, beta frequency fits reasonably well resonant activity within more localized circuits.

*2.1.4.4. Gamma activity*

Oscillations and synchrony in the gamma band (20 - 70 Hz), especially 40 Hz oscillations, are strongly related to cognition in which conscious perception and control plays a part. Perhaps the most well known indication of this relationship is the 40 Hz activity during REM sleep (Mendel & Goldstein, 1971). In delta sleep (see section 1.1.4.1), both gamma activity and dreams are absent. Awake subjects show a 40 Hz response to auditory stimuli that is absent during a certain kind of anaesthesia (Madler et al., 1987).

Gamma activity not only differentiates general states of arousal. Complex motor actions result in synchronous gamma activity in monkey motor and somatosensory cortex that is weaker during simple actions (Murthy & Fetz, 1992). EEG and MEG studies (Kristeva-Feige et al., 1993; Pfurtscheller et al., 1994) show increases in gamma activity prior to complex movements in humans.

Coherent visual stimuli such as Kanizsa triangles (three pac men with their mouths creating the three points of a "white" triangle) (Tallon-Baudry et al., 1995) and

moving lines (Lutzenburger et al, 1995) result in gamma activity over visual cortex, while incoherent stimuli with equivalent elementary visual characteristics (pac men turned away from each other, lines that do not move as a group) do not. The Lutzenburger study also showed that the oscillations occur at the specific locations in the brain activated by the stimuli: inferior and superior occipital sites respond to stimuli in the upper and lower visual fields respectively. The gamma activity related to auditory stimuli was noted above. Sequences of clicks with a driving frequency around 40 Hz have the added property of increasing power at the sequence's frequency.

Finally, gamma activity is clearly related to word processing. Visually (Lutzenburger et al., 1994) and auditively (Pulvermüller et al., 1995) presented words resulted in stronger 30 Hz activity, located specifically over left perisylvian cortex, than pseudowords. In a lexical decision task, Pulvermüller et al. (1996) showed that the processing of verbs was related to 30 Hz activity over motor cortex whilst processing nouns resulted in 30 Hz activity over visual cortex.

In a review article, Tallon-Baudry and Bertrand (1999) note that the spatiotemporal characteristics of gamma activity depend on the task and on which sensory areas are used, and that an interpretation in terms of dynamic linking mechanisms fits well with these characteristics. Three studies directly concerned with synchrony provide preliminary support for this interpretation, the assumption being that phase-locking (see section 1.2 for details) is unlikely to occur without some kind of direct relationship. The first is that by Engel, König and Singer (1991) described above. Lachaux et al. (1999) found synchrony around 40 Hz between various brain areas using intracortical measurements in an oddball task. Haig et al. (2000) also used an oddball task, and found global increases in EEG synchrony around 40 Hz and synchrony between electrodes within large regions.

It appears that the various frequencies at which activity occurs in the brain may have quite clear functional distinctions. Delta activity represents inhibition; alpha activity the (lack of) influence of local interactions on local activity; beta activity the local non-transient connectivity of neural networks; and gamma activity grouping and transient connectivity between specialized areas. Despite the variety in functions, they

can be explained by a small set of underlying mechanisms: coincidence detection, neural network interactions and transient connectivity.

The theories and results discussed in the preceding sections show the importance of oscillatory activity in the brain. They help to understand how binding may be realized in the brain and provide a first step in determining how the formation of cell assemblies at various scales may result in local - global interactions. Examples are the global-to-local process of tonic depolarization and the local-to-global process of cell assembly recruitment. The psychophysiological information provided by oscillation and synchrony studies, together with general theories of oscillation and synchrony such as those provided in sections 1.1.1 to 1.1.3 or by Nunez (2000), may be used in the construction of detailed hypotheses concerning the measurement of predicted instances of cell assembly activation, inhibition, local network interactions and transient connections. However, more elaborate and specifically cognitive models are required to provide such predictions. Such models must specify how the neuronal representations of goals and memory create the global and local conditions under which synchrony results in controlled, coherent behavior.

*2.1.5. Synchrony and selection for action*

The following theories and models may help to predict when and which patterns of synchrony will occur, and to interpret those patterns if they are found.

Fuster (1997) bases his model of the brain on the perception – action dichotomy in mammalian neurology, in which anterior and posterior areas are concerned with action and perception respectively. The required temporal integration of action (both motor and cognitive, such as attention) is provided by prefrontal cortex. Moscovitch' (1992) model of memory and consciousness contains three components: the posterior, temporal and frontal lobes. Posterior areas contain specialized functional units, of which only the output and input are available to consciousness and conscious control. Temporal medial areas are the location of automatic memory storage and retrieval, such as that due to cueing. The frontal lobes receive output from the other two components and support strategic, controlled encoding and retrieval processes. The functions performed by the frontal lobes are termed working-with-memory. Damasio and Damasio (1994) provide neuropsychological evidence that memory is a process in

which early sensory and motor cortices become activated as part of an ensemble. Anterior convergence zones, ensembles of neurons at the nexus of many feedforward and feedback connections, play the organizing role in Damasio and Damasio's model of memory. In all these models specialized posterior neuronal groups with relatively simple functions are organised by anterior areas to achieve more complex representations and cognition.

Switching between tasks is an example of temporal organization of interest to this study. An aspect of task switching we expect to be susceptible to study by the EEG methods described in section 1.2 is selection for action.

Simon (1994) points out the ecological necessity for the human organism to have both parallel and serial functions. Selection for action is concerned with the parallellity of information in the brain, which must somehow result in effective serial actions in the outside world. The transient connection of relevant neuronal representations to anterior areas is the neuronal expression of selection for action suggested by the functions of synchrony and the models described above. More specific predictions for these anterior areas are given by Burgess et al. (2000).

Burgess et al. provide neuropsychological evidence for the location of three components of multitasking: retrospective memory, prospective memory and planning. The respective areas are the posterior cingulate, Brodmann areas 8, 9 and 10 (tentatively) and the right dorsolateral prefrontal cortex. Note that the location of retrospective memory, that is, the location of its organizing area, is neither anterior nor, in fitting with Fuster, action - directing. However, the connections within retrospective memory represent the task instructions to be followed and are thus an important part of multitasking and task switching.

The models introduced above allow us to formulate hypotheses concerning at least some of the processes of switching between tasks. These hypotheses, concerning synchrony measured between EEG channels, will be discussed in section 1.3.

## 2.2. Measuring synchrony

The following section is concerned with the measurement of synchrony at the scalp. First, the decomposition of a signal using wavelet analysis will be discussed. This decomposition is used in a number of measures of synchrony, two of which will be described in section 1.2.2. Two other measures we will not discuss are coherence and quasi-coherence. These measures are based on both phase and amplitude, and were dropped in favour of the measures of section 1.2.2, which are based only on phase relations. Finally, we will look at problems caused by the way signals from the brain translate into electrical fields that can be measured at the scalp, and, where available, solutions for these problems.

*2.2.1. Wavelet analysis*

Fourier analysis is based on the theorem that any signal can be written as the sum of sines and cosines of various amplitudes (the peak of the function) and phases (the shift of the function along the ordinate) (Glaser & Ruchkin, 1976). Wavelet analysis determines the amplitude and phase, not of component (co-) sines of specific frequencies, but of component *wavelets* with a frequency and temporal content centred on various values. An example of a wavelet (the Morlet wavelet) is given in figure 1.2. Note, first, that the wavelet is localized in time: the further points are from the centre, the more their function values approach zero. This is not the case for sines, which keep on oscillating with the same amplitude to plus and minus infinity. Second, a sine is precisely localized in frequency, whereas the wavelet has a frequency mean around which its amplitude decreases with distance.

*Figure 1.2. Temporal and frequency characteristics of a wavelet*

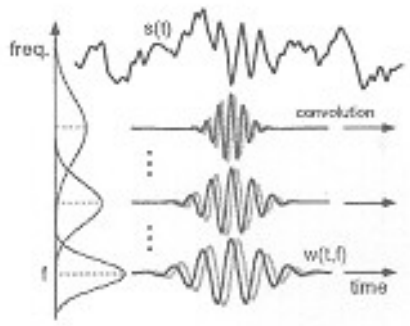


*Taken from Tallon-Baudry & Bertrand (1999).*

There are infinitely many wavelets, just as there are infinitely many sines. However, all wavelets are localized, like the example, in time and frequency. This localization is not exact. There is always a range in either time or frequency or both around the mean over which the amplitude of the wavelet decreases to zero (Raz, Dickerson &

Turetsky, 1999). The amplitude of the Morlet wavelet, the wavelet we use in our analyses, is a Gaussian function in both time and frequency centred on the mean, and the relationship between the amplitude function in time and frequency is always

$$\sigma_f = 1 / ( 2\pi * \sigma_t )$$

where $\sigma_f$ and $\sigma_t$ are the standard deviations of the amplitude function in frequency and time, respectively. The standard deviation of a Gaussian function determines its width, higher standard deviations corresponding to a broader curve. The resolution of a wavelet, that is, the specificity of the kind of signals it responds to (see below), is directly related to its $\sigma_f$ and $\sigma_t$. The $\sigma f$ is also central to the definition of wavelet families. Wavelets belonging to the same family all have the same $f / \sigma f$ ratio, the wavelet parameter.

In Fourier analysis the influence of all components of the signal with a frequency unequal to that of the chosen (co-) sine is zero. In wavelet analysis, components of the signal around the mean of the wavelet also contribute to the results, and hence the resultant amplitude and phase, due to the nonzero amplitudes around the mean frequency. This is what was referred to above as the wavelet responding to (components of) signals with frequencies around its mean frequency, not specifically to signals with exactly its mean frequency. The exception to this lack of specificity in frequency is when $\sigma_f = 0$, in which case $\sigma_t$ = infinity, and the wavelet becomes a (co-) sine. The analogous exception is infinite lack of specificity in frequency, where all the signal components are lumped together and the well-known time – amplitude signal is returned.

The advantage of using wavelets over the (co-) sines in Fourier analysis is the localization in time of the former, which is "paid for" by their lack of specificity in frequency (Raz, Dickerson & Turetsky, 1999). The trade-off between specificity in time and frequency is a choice of the researcher, allowing for a flexible approach based on the type of data and experimental objectives. The advantage of wavelet analysis over Fourier analyses done on sections of signals is that the latter analyses require a choice of fixed window, which will only be optimal for detection of

waveforms at one time scale. Wavelet analysis offers variable windows, where faster rhythms in the same family are inherently more localized in time due to the constant $f / \sigma_f$ ratio and $\sigma_f = 1 / (2\pi * \sigma_t)$ equation. Samar et al. (1999) note that this leads to the possibility of handling both large- and small-scale structure by a single, efficient analysis protocol.

If the $\sigma t$ is nonzero, adjoining time points will produce largely redundant information, so in the method used in this study not all time points were analysed. The analysed time points were taken in steps of the smallest $\sigma_t$ used in the analysis. As well as reducing computation time for the wavelet analysis itself, this procedure will turn out to reduce statistical and computational problems in later stages of analysis.

Wavelet analysis is based on the convolution of a signal with wavelets, where, depending on the $\sigma_t$, only the part of the convolution centred on the mean-in-time of the wavelet will be (practically) nonzero. However, the amplitude and phase of a signal component of a given frequency at a certain time can also be extracted by complex demodulation, which is faster and provides equivalent results.

*2.2.1.1. Complex demodulation*

The aim of complex demodulation is to extract the time course of the amplitude and phase of a perturbed periodic component in a signal. Such a component can be written as

$$x(t) = R(t) * \cos(\lambda t + \Phi(t))$$

in which R(t) is the amplitude as a function of time and $\Phi(t)$ is the phase shift as a function of time ("perturbation" refers to the amplitude and phase being a function of time, not constant over the whole series). Complex demodulation is characterized in Bloomfield (1976; this section is largely based on chapter 6 of Bloomfield's book) as a local version of harmonic analysis, where the amplitude and phase at time t are determined only by data in the neighborhood of t, not by the whole series.

Complex demodulation is based on the convolution of $x_t$ with an *analysis oscillator* term, exp(-iλt), where i is sqrt(-1). This analysis oscillator is set to the frequency of interest through the choice of λ. The convolution is now rewritten using the following formulae:

1. y(t) = x(t) * exp(-iλt).
2. x(t) = R(t) * cos(λt + Φ(t))
   <=> x(t) = ½ * R(t) * [exp(i(λt + Φ(t))) + exp(-i(λt + Φ(t)))],
   because exp(i*$x$) = cos($x$) + i * sin($x$), where $x$ = λt + Φ(t) and thus the term between square brackets can be rewritten as

   cos(λt + Φ(t)) + i * sin(λt + Φ(t)) + cos(λt + Φ(t)) - i * sin(λt + Φ(t))
   = 2 * cos(λt + Φ(t)),
   which must then be divided by two to recreate the original cosine.

Inserting 2) into 1) produces

3. y(t) = ½ * R(t) * [exp(i(λt + Φ(t))) + exp(-i(λt + Φ(t)))] * exp(-iλt)
   <=> y(t) = ½ * R(t) * exp(iΦ(t)) + ½ * R(t) * exp(-i(2λt + Φ(t))

The first term of this final form of y(t) can be used to calculate the desired time series:

4. In y(t) = ½ * R(t) * exp(iΦ(t)), R(t) is twice the norm of y(t), as the right side of the equation is simply the exponential form of a complex number. The norm of y(t), and hence R(t), can be calculated by writing y(t) = x(t) * exp(-iλ) as y(t) = x(t) * cos(λt) - i * x(t) * sin(λt), of which the norm is simply the square root of [x(t)² * cos(λt)² + x(t)² * sin(λt)²]. The phase at time t is the arctan of -(x(t) * sin(λt)) / (x(t) * cos(λt)), as can be seen by drawing y(t) as a vector.

The second term must thus be removed, as well as, in realistic data, a noise term z(t) which in the convolution y(t) becomes z(t) * exp(-iλt). The result of these removals, that is, the first term, is called the demodulated series. Demodulation, the process of

removing the second and third term, is based on the smoothness of the first term: note that due to the fact that the analysis oscillator is exp(-λt), the λt disappears from the first term in the convolution. The functions in the goniometric form of the first term now do not contain a λt argument any more, or more formally, the λ is zero. The second term oscillates around –2λ Hz and the third term cannot be smooth as all frequencies of λ are regarded to be part of the first component, so the noise component by definition cannot contain those frequencies which would be shifted to zero frequency.

Due to the smoothness properties of the terms, linear filtering can be used to separate the first component from the other two components, providing the necessary demodulation. Linear filtering will not be described in detail here, but is based on the idea of taking a running average of adjacent points. Because smooth components will be roughly the same over adjacent points and noise will vary with mean zero, the result of such a running average will represent the smooth signal more than the noise. The details of linear filtering are concerned with the choice of weights for the running average. Note that this subsequent application of linear filtering makes the equivalence of wavelet analysis and complex demodulation understandable at an intuitive level, as the function values of a Morlet wavelet are themselves the product of an analysis oscillator and a weighted average.

*2.2.2. Using the phase results of wavelet analyses to define and detect synchrony*

Section 1.2.1 provides us with a more precise definition of synchrony: a consistent phase-difference between two signal-components centred on a given frequency band around a certain point in time.

After a completed wavelet analysis, every analysed time point of every signal has been assigned a value for the instantaneous amplitude and for the phase of its surrounding signal in a number of frequency bands chosen by the researcher. The measures we used for synchrony were based on the phase data. The first measure we will discuss is the phase-locking value (PLV, Lachaux et al., 1999). The second, the quasi phase-locking value (QPL, de Jong, 2000), is a variant of the PLV sensitive to a somewhat different kind of order in phase relations.

*Figure 1.3. Consistent and inconsistent phase difference vectors and their average*

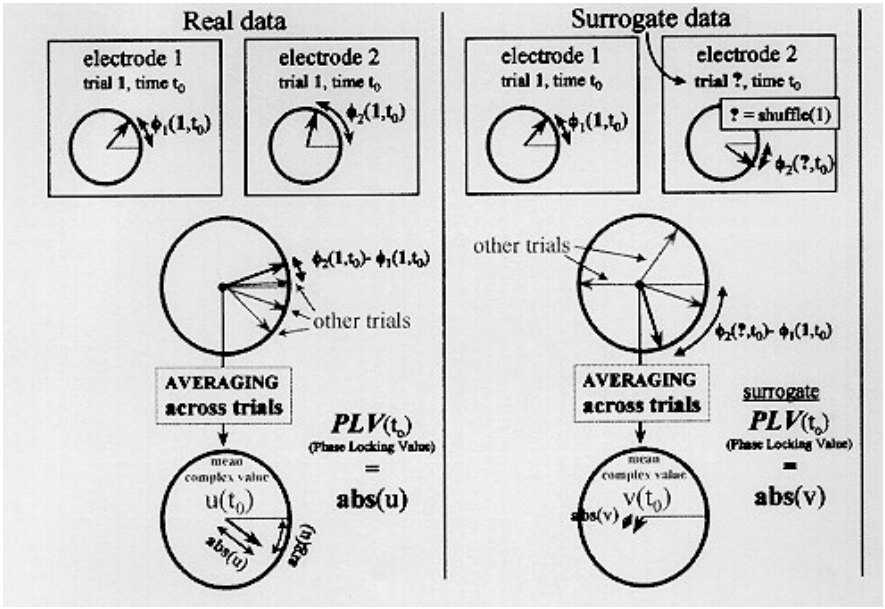


*Taken from Lachaux et al (1999). The left and right examples show a consistent and inconsistent phase difference respectively. The average vector is longer for the consistent differences than for the inconsistent ones.*

The phase-locking value (PLV, Lachaux et al., 1999) measures the consistency of the phase difference between two signals, around a given time point and frequency, over trials. The PLV is defined to be

$$PLV(t) = (1 / N) * | \Sigma n \exp (j * (\varphi 1(t, n) - \varphi 2(t, n)) |$$

The reasoning behind this measure is as follows. Consider the phase difference of every trial at the time point and frequency of interest as a normalized vector within the unit circle. The example in figure 1.3 shows two conditions, one with consistent and one with strongly varying phase differences. Add the vectors head-to-tail and divide the length of the sum-vector by the number of trials. As illustrated in the examples, if the phase differences are consistent over trials, the length of this average vector will approach unity as the aligned vectors build up to a long, more-or-less straight vector, and if the differences are random the average will approach zero as the vectors will tend to cancel each other out.

The precise formula for the PLV is a formalization of this procedure. Exp (jx) = sin(x) + j * cos(x), where the sine and cosine parts of the equation can be mapped to

the x and y axes of the unit circle and thus can be represented as vectors. Taking the norm of these vectors removes the imaginary component.

The PLV only assigns high values to time points at which the specific phase difference is consistent over trials. This means it will not detect synchronies if the phase difference differs over trials. Note that this does not mean there is no synchrony: even if the phase difference is not consistent over trials, it may be consistent over time points within trials. For example, on trial *i* two areas may show a phase-locking with 45 degrees difference around some latency, whereas on trial *i*+1 the phase-locking may occur around the same latency but with 10 degrees difference. Our second measure, the QPL, was designed to detect this kind of consistent phase-locking in the absence of consistent phase differences. The QPL is computed as follows:

1. Select a number of adjacent time points as a segment of a trial. We used the samples within +/- 4 * $\sigma$t ms around the mean time.
2. Compute the intra-trial PLV over the time points of the segment. The values are weighted by the Gaussian curve for the localization in time. Due to the smoothing effect of the wavelet (adjacent wavelets are largely based on the same set of samples), the intra-trial PLV will show an artefactual synchrony. However, as we are interested in changes over time and the artefactual synchrony is constant over time points this does not present a problem.
3. Repeat 1 and 2 for every trial.
4. Average the intra-trial PLV over all trials for the QPL value.

Note that the value per trial is abstracted from the specific phase difference to the intra-trial PLV before averaging over trials.

*2.2.3. Measuring brain synchrony at the scalp: problems and solutions*

The signals of interest in this study are of course EEG waveforms. However, the synchronies of interest are those between groups of neurons within the brain. This relationship between signal and source is complex and presents a number of problems.

First, we will discuss the route from neuronal activity to electrical currents at the scalp.

*2.2.3.1.Field potentials generated by neurons*

Neurons generate electrical fields because of the flow of ions through cell membranes, as during action potentials (transmission of current / information within a neuron) and post-synaptic potentials (transmission of current / information between neurons, Allison et al. (1986)). Two types of currents are generated during an action potential. First, there is a current along the axon, as the action potential travels away from the soma. Second, the action potential causes local currents due to the ions travelling in and out of the cell. This second kind of current produces a field that is negative above the location of the action potential (a current sink) and positive at some distance towards the soma and the axon terminal (current sources). Current sinks and sources are the only type of field generated by post-synaptic potentials, and produce stronger fields than the movement of the action potential (Allison et al, 1986).

The potentials generated by several currents summate at all locations in extracellular space (this is Helmholtz's principle of superposition, Allison et al., 1986)). The orientation of nerve cells determines whether their fields will be measurable at a distance. Open fields (parallel alignment) do, and closed fields (dendrites radially extending outwards from a central group of neurons) do not produce measurable fields. Ring-dipoles are a less well-known configuration possibly important to synchrony (Tallon-Baudry, 1999).

*2.2.3.2. Eight problems*

Allison, Wood and McCarthy (1986) list the following seven limitations of surface ERP's in psychophysiological research. Note that they themselves do not present them as fundamental, insurmountable or even unsolved, and supplied some of the answers presented in the next section. Also note that the problems and answers presented below are based on the generation of the EEG the ERP is based on, not the averaging process. As the PLV and QPL are based on the same EEG as the ERP, the discussion below also applies to those measures.

1. The scalp ERP is a summation of all the currents produced by active neurons; it is a statistical aggregate in which it is unclear which neurons have contributed what.
2. The ERP only represents the activity of neurons with certain characteristics concerning orientation, location and synchrony.
3. There is no one-to-one relationship between psychological processes and ERP components.
4. Even well-defined and precisely localized ERP components would not imply anything about the nature of the information processing operations they represent.
5. The polarity of ERP's can not be used to draw conclusions about the underlying neurophysiological basis.
6. Potentials from different sources may overlap in time and space.
7. The brain structures responsible for an ERP may not lie directly under the scalp region where the ERP's amplitude is maximal.

We add problem 8, a specific consequence of problem 1 especially relevant to research on synchrony:

8. The spatial resolution of recordings at the scalp is low. Measures taken from different points, especially points closer to each other than about 10 cm may largely represent the same underlying activity (Nunez, 2000), leading to artefactual synchrony.

*2.2.3.3.Six answers*

Now we will consider some answers to these problems.

1. Source localization combined with methods like fMRI and background anatomical knowledge allow the likelihoods of various numbers and locations of dipoles underlying scalp potentials to be investigated. (problems 1 and 7).
2. The selectivity of the brain activity picked up by the EEG has its advantages. Knowing what brain structures were unlikely to have contributed to the EEG attenuates the problem of source localization in

general, and only having to deal with a subset of activity makes the problem space a little smaller. Furthermore, it may be that it is the activity that can be picked up, e.g. of pyramidal cells, is of more theoretical interest than the activity that cannot, in which case the signal-to-noise ratio of relevant information would be enhanced (problem 2).

3. Computational theories supply component processes which may be more easily mapped to specific ERP components than the emergent processes such theories explain. Problems in relating psychological functions to ERP's whilst those psychological functions are not even specified at the same level of detail in time as the ERP's are obviously to be expected, and say less about the limitations of the technique than the inadequacy of the theories (problem 3).
4. It is psychological theory that conveys meaning to any experimental variable, including ERPs. However, phase-locking does perhaps have more inherent meaning due to the theories presented in section 1.1, which may have a positive effect by guiding interpretation (problem 4).
5. Experimental design can help distinguish ERP components reflecting different information processing operations. This implies that the necessary unit of experimentation needed to identify ERP components despite the overlap in time and space and the complexity of ERP - function relationships is not a single experiment, but a combination of experiments, working together to identify components which do not overlap in *condition* (problem 6).

Problem five stands as a caveat, especially when interpreting oscillations. Alternating positive and negative currents are not necessarily caused by two open-field groups of neurons perpendicular to the scalp alternately firing action potentials at each other (for an example of another possibility see Allison, Wood and McCarthy, 1986, p. 15).

These answers are satisfactory to varying degrees, but do seem to imply that the limitations of scalp recordings may be solved or compensated for, to some extent at least.

The sixth answer, a possible solution to problem 8, is current source density (CSD) analysis, the subject of the next section.

*2.2.3.4.Current Source Density analysis*

This section is largely based on Nunez (1981). Because the skull is a bad conductor, current sources and sinks will only be measurable if they are due to neuron groups perpendicular to the skull. Most locations on the scalp would not have perpendicular current sources / sinks directly underneath them. However, the raw EEG data consists of electrical potentials, which are present at locations other than those directly over the current sources. Current source density (CSD) analysis (Perrin et al., 1989) uses the potential data to calculate a measure that reflects the density of the current sources below the skull.

Before explaining the CSD procedure, the concept of current density should be explained. The total current in an electrical circuit is uniform at all location in the circuit, but this is not the case in the brain. A more useful measure is current density, the current flowing through the cross-section of a certain volume in the brain. The formula for current density is $\Sigma \rho * v$. $\rho$ is the charge density: the number of free ions of a certain charge in the volume multiplied by their charge, the unit being $C / m^3$. v is the average vector [m / sec] of the velocity of these ions. The summation is over all types of ions and results in the current density [$C / (sec * m^2)$ or $A / m^2$]. Current density is highest where the density of sources of current, dipoles in the simplest case, is high. As stated above, CSD detects this density of current sources.

Obviously, the $\rho$ and v terms are unknown, but it will now be shown how the relevant current information can be derived from scalp potentials.

At locations not above a current source / sink, the current density function will be flat over the sphere of the scalp, only showing steepness where the current density is high. The two-dimensional first derivative of the current density is thus a suitable measure for locating underlying current density sources. The following equations show how this measure is related to the scalp potential.

1. $\nabla J = \partial Jx / \partial x + \partial Jy / \partial y$, where $\nabla$ is the two-dimensional first derivative or deviation and J is the current density.
2. $J = \sigma E$, where $\sigma$ is the conductivity and E is the electrical field.
3. $E = - \nabla \Phi$, where $\Phi$ is the potential

Now insert 2) into a variation of 1) to get

4. $(-1 / \sigma) * \nabla J = (- 1 / \sigma) * \nabla \sigma E$

$\Leftrightarrow \quad (- 1 / \sigma) * \nabla J = -\nabla E$

Finally, insert 3 into 4 for

5. $(- 1 / \sigma) * \nabla J = -\nabla -\nabla \Phi$

$\Leftrightarrow \quad (- 1 / \sigma) * \nabla J = \nabla^2 \Phi$

Thus, the first derivative of current density is proportional to the second derivative of the scalp potential.

The method of calculating the current density consists of two steps. First, the scalp potential is calculated from the discrete electrode positions and values. The software we used, Brain Vision, calculates splines (a spline is a type of curve; see our explanation of splines in section 2.5 for more details) that smoothly interpolate the electrodes. This calculation requires two parameters: the order of the splines, which is analogous to the smoothing parameter described in section 2.5 and determines the flatness of the curve, and the maximum degree of the Legendre polynomials used to calculate the splines. The maximum degree determines how many component polynomials are used to approximate the spline. A flatter spline requires fewer component polynomials to be reasonably approximated, hence the rule of thumb that a higher order of splines should lead to choosing a lower maximum degree of Legendre

polynomials. Second, the second derivative of the continuous potential field of the first step is calculated.

Current sources and sinks are more localized than the overall current they cause, so CSD data would be expected to have a better spatial resolution than EEG data. This is supported by experiments, e.g. Nunez (1981).

## 2.3. Possible roles of synchrony in switching between and maintaining task sets

### *2.3.1. The task-switching paradigm*

The average reaction times for tasks when subjects have to alternate between them are longer than those for the same tasks if performed in isolation (Jersild, 1927). The extra time caused by the alternation is referred to as a switch cost. The task-switching paradigm is an experimental framework in which subjects must alternate between tasks. We will use Roger & Monsell' s (1995) alternating runs paradigm to illustrate the most important characteristics of the paradigm.

In Roger & Monsell's task, blocks of trials consist of a sequence of a pair of one task followed by a pair of another. Labelling the different tasks A and B, this results in an AABBAABB... trial sequence. In this design two conditions can be distinguished: a switch condition consisting of trials following a trial in which a different task had to be performed (respectively the A and the B in BA and AB sequences), and a nonswitch condition in which the present and the preceding tasks were the same (the second trial of the AA and BB sequences). The difference between the reaction times on switch and nonswitch trials is the switch cost.

The time a subject is given to prepare for the subsequent trial is an important variable in this paradigm. This time is calculated as the interval between response and the next stimulus (the response-stimulus interval, RSI). Rogers and Monsell (1995) describe preparation as the subject-driven creation of a new mapping of stimuli to responses; a specific mapping is called a task set and changing task set, either prior to or after stimulus presentation, is called task-set reconfiguration. Sohn et al. (2000) modeled preparation in ACT-R (Anderson & Lebiere, 1998), a theory of cognition concerned with the goal-directed retrieval and application of information, as the active retrieval of task relevant knowledge. In the intention-activation account of task-switching (de

Jong, 2000), subjects must have the intention, or goal, of preparing for trials, and retrieve and carry out that intention prior to stimulus presentation. So, in endogenous preparation, the subject must want to prepare for tasks (in terms of ACT-R, the goal of preparation must be active), recall that a change in task will occur, retrieve the relevant task-knowledge prior to trials, and in doing so activate the specific stimulus-response mappings necessary to correctly perform the new task.

*Figure 1.4. An example of switch costs*

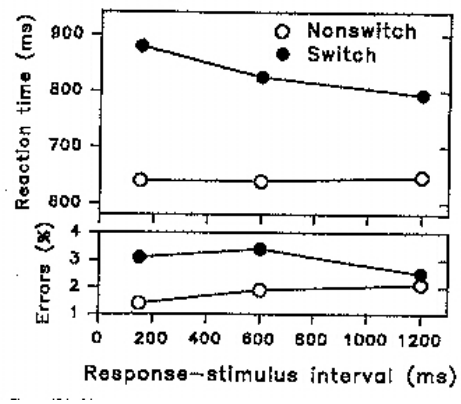


*Taken from de Jong, 1995*

As can be seen in figure 1.4, switch costs gradually diminish as the interval provided for preparation is prolonged, indicating that subjects are able to prepare for switch trials. As RSI is not related to the reaction time on repetition trials, preparation does indeed seem to be specifically concerned with changing task-set. The switch costs at the longest preparation interval are called residual switch costs, because ample time is provided to complete any endogenous preparation.

*2.3.2. Theories concerning residual switch costs*

The following explanations of residual switch costs will be discussed in the next sections:

1. The task-set inertia hypothesis

2. The task-set reconfiguration hypothesis

3. The failure-to-engage hypothesis

*2.3.2.1.Task set inertia (TSI)*

Allport et al. (1994) attribute switch costs to some kind of proactive interference, which they call task-set inertia, due to the same stimuli being used in competing

stimulus – response mappings. The mappings persist from the instruction set on previous trials and therefore interfere with the instruction set on the next trials. The switch costs are not considered to be the result of central executive processes, but are caused by the time taken by the information processing system to settle into a unique response to the next stimulus. In the Norman and Shallice (1986) model of conflicting schemata, this is the process of sorting out which schema is probably best suited to take control of action. The TSI hypothesis thus states that switch costs represent an automatic, stimulus-driven process.

*2.3.2.2.Task set reconfiguration (TSR)*

The task-set reconfiguration hypothesis by Rogers & Monsell (1995) states that switch costs measure the duration of a process of enabling and disabling connections between processing modules, and / or re-tuning the input-output mappings performed by these processes, so that the same type of input can be processed in the different way required by the new task. Whereas Allport et al. suggest that switch costs arise solely from automatic processes, Rogers & Monsell propose that there is also an endogenous component involved: advance preparation by the participant also influences reaction times.

Advance preparation, as described above, is an anticipatory process initiated by subjects in order to prepare for a predictable switch. This endogenous component can reduce switch costs if the participant is given enough preparation time to complete the reconfiguration process, but can never eliminate the costs of switching tasks as these costs also reflect an exogenously triggered component. This second component is triggered by stimuli and involves competition between two S-R mappings, as in the TSI hypothesis. Although Allport et al. suggest that this competition between S-R mappings can be noticed several trials after a switch, Rogers & Monsell found in experiments that this process is better described as a one-off task-set reconfiguring process.

*2.3.2.3.Failure-to-engage (FTE)*

The failure-to-engage hypothesis is based on the assumption that subjects can fully prepare during the RSI but sometimes fail to engage in full advance preparation. That

is, the intention described in 1.3.1 is not activated. Switch costs are attributable to the effect of unprepared trials on the average reaction time.

The mixture model of de Jong is based on the FTE hypothesis. A first step in using the mixture model is the calculation of cumulative distribution functions (CDFs) by dividing the rank ordered RTs for each subject, for each condition into deciles (10% bins) and then computing the mean RT for each bin. Figure 1.5 shows that the responses on the switch trials with the longest preparation interval can be seen as a mixture of two basic types. Responses in the nonswitch condition of the long preparation interval should be relatively fast and can be regarded as responses in a prepared state, because the task set is already configured. Responses in the switch condition of the shortest preparation interval should be relatively slow and can be regarded as responses in an unprepared state, as the time given is too short for advance preparation and the task-set reconfiguration is incomplete. Now, the reason the CDF for the switch, long RSI condition suggests a mixed distribution of prepared and non-prepared responses is that when the responses are fast, they are as fast as the nonswitch (prepared) condition and when they are slow, they are as slow as the switch, short RSI (non-prepared) condition.

*Figure 1.5. Cumulative distributions*

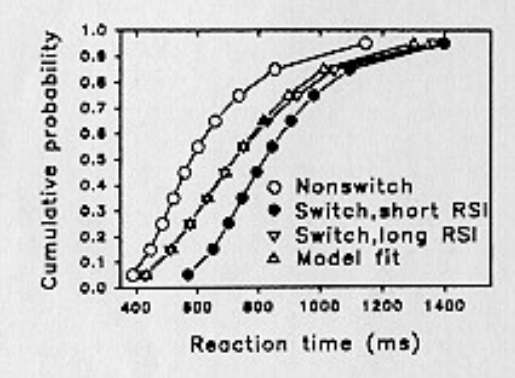


*Taken from de Jong (2000).*

The CDFs illustrate the FTE hypothesis that switch trials with a long preparation interval can be seen as a mixture of responses with a completed task set configuration and responses where subjects failed to prepare in advance. This description is shown by the following equation, in which F is the CDF-function:

$$F_{\text{switch, long PI}}(t) = \alpha\, F_{\text{prepared}}(t) + (1 - \alpha)\, F_{\text{unprepared}}(t).$$

The α in this equation is the mixing probability: the probability that advance preparation is carried out completely during the long preparation interval. The

estimates of the prepared and unprepared RT' s are, respectively, the RT' s on the nonswitch trials with a long preparation interval and the RT' s of the switch trials with a short preparation interval. This provides the following equation:

$$F_{switch,\ long\ PI}(t) = \alpha\ F_{nonswitch,\ long\ PI}(t) + (1 - \alpha)\ F_{switch,\ short\ PI}(t).$$

If the prepared and unprepared CDFs have the same shape, but are shifted in time, including an extra, time-shifting parameter δ would provide a better fit. The δ can be seen as a reflection of an exogenous component of task-set reconfiguration which, under the FTE hypothesis, should not provide a benefit over the model with only the α parameter.

$$F_{switch,\ long\ PI}(t) = \alpha\ F_{nonswitch,\ long\ PI}(t - \delta) + (1 - \alpha)\ F_{switch,\ short\ PI}(t).$$

So, if switch costs arise purely from the fact that, on switch trials, the average RT is based on two underlying distributions, the δ would be zero and the α sufficient to describe the overall CDF. If the CDF for long switch trials is simply based on the RTs of long nonswitch trials plus the time taken for an extra process, the α will be 1 and the δ will indicate this extra time. The α and δ parameters can be estimated by using the multinomial maximum likelihood model (MMLM (Yantis, 1991)). The measure in which FTE determines a reaction time distribution can be evaluated by testing the fit of the restricted model (α only) and then either testing whether generalizing the model by including the δ parameter significantly improves the fit, or testing whether the δ parameter of the generalized model is significantly different from zero. The second of these methods is preferable, because the a priori distribution of the $G^2$ statistic is unknown in the generalized model.

*2.3.3. Hypotheses on task switching and synchrony*

Numerous studies have already validated the basic idea of the mixture model (e.g. Lorist et al., 2000): the RT distribution for switch trials is bimodal, consisting of the overlapping prepared and unprepared distributions. Our hypotheses are concerned with the physiological processes leading to the different reaction times.

To our knowledge, no psychophysiological studies have been performed using the prepared – non-prepared difference. The literature does provide some indications of which brain areas may be relevant for preparation. Dorsolateral prefrontal cortex has been related to various kinds of cognitive control (Sohn et al., 2000: holding items in working memory (Cohen et al., 1997), dual task performance (Courtney et al., 1998), switching between task dimension (Konish et al., 1998) and switching to a cognitively more demanding task (MacDonald et al., 2000). Superior parietal cortex has been related to the allocation of attention (Corbetta et al., 2000), being more activated during the cueing period of a spatial cueing paradigm (MacDonald et al., 2000). fMRI studies have shown that switch trials (both pre- and post-stimulus) are associated with higher levels of activation than repetition trials (Kimberg et al., 2000; Sohn et al., 2000; Dove et al., 1999). The same studies suggest that prefrontal and parietal areas may be specifically concerned with task-switching, regardless of which tasks are being switched between. Sohn et al. explicitly distinguished endogenous and exogenous components of switching by manipulating foreknowledge of the task to be performed. Endogenous preparation, where foreknowledge was used during the preparation interval, was related to higher activation in inferior lateral prefrontal cortex and superior posterior parietal cortex. Exogenous adjustment, which must occur after stimulus presentation on trials without foreknowledge, was associated with superior prefrontal cortex and posterior parietal cortex. Under the FTE hypothesis, exogenous adjustments when foreknowledge is available are consequences of failures to engage.

In section 1.1.5, selection for action was introduced as a task-switch component in the working with memory model. The task set must determine which stimuli or stimulus attributes will be attended to, and to which response they will be mapped. Our hypothesis is as follows: the successful reconfigurations during the RSI preceding prepared trials involve transiently connecting the places where stimuli will be represented to the correct responses, whereas this linking will not occur before unprepared trials. The TSR hypothesis suggests that an old task set may be visible in both cases, preparation replacing its obsolete patterns of synchrony with new connections.

This study is exploratory, but we were especially interested in the following possibility. Transients connections seem likely to arise during the reconfiguration process and after successful initiation of a task set, and these may be detectable via wavelet analyses as synchronies, especially between relevant perceptual and prefrontal and / or (pre-) motor areas. The tasks we used were therefore chosen to recruit well-separated brain areas, in consideration of the limitations of the EEG technique, and will be described in the method section.

# 3. Method

## 3.1. Subjects

Twelve right-handed subjects, aged 18-30, participated in this study. All of the subjects had normal or corrected to normal vision. None used any psychoactive medication. Six subjects were lost due to technical difficulties and unsuitable response characteristics (very high or low α' s).

## 3.2. Procedure

The tasks used in the experiment were a rhyme task and a visual task, programmed in MEL and presented on a 17'' Brilliance 107 MP monitor 80 cm away from subjects. Both tasks used the same stimuli, which were presented inside one of four cells in a 2 by 2 matrix. The matrix was 15 by 9 cm, corresponding to +/- 5,3 and +/- 3,2 degrees for the visual angle. The used cell rotated one step clockwise each trial. The stimuli were composed of a single-digit number and a word, presented in different intensities one above another. The words were real and pseudo-words and all rhymed with the spoken sound of a number from one to nine. Intensity was based on the red-green-blue values of which colours can be composed in MEL (the values for each of the three colours were integers running from 0 to 64) at a monitor intensity setting of 50%. Letters and numbers were presented in a 0,8 by 1,2 cm font. Stimuli remained on screen until a response was given and the next stimulus appeared after a response-stimulus interval (RSI), which could be 100, 750 or 1500 ms.

In the rhyme task, subjects had to decide if the stimuli rhymed, while in the visual task they had to decide if the stimulus with the highest intensity occupied the upper location. Rhyming stimuli were those such as "7 heaven" or "1 gun". The difficulty of the visual task was adjusted during performance by changing the relative difference between intensities of the stimuli in an attempt to keep average reaction times of both tasks similar. The added intensity of the more intense stimulus was determined as an intensity parameter times the ratio of the lower intensity divided by the maximum intensity. The intensity parameter was adjusted based on the difference in reaction times of the past twenty trials. If the difference was larger than 5 % an adjustment of the intensity parameter of 0.1 was made. No reduction of the difference was made if an error had been made during the considered trials, and trials with reaction times

below 200 or above 2000 ms were not used for determining intensity adjustments. Per block (see below) the intensity parameter was not permitted to change more than 2 points.

The response keys were the Z and X for the left hand and the M and N for the right hand. The mapping of the keys to "yes" and "no" responses was random over subjects. At the beginning of the experiment the assignment of a task to a particular hand was chosen at random. This assignment was switched halfway through the experiment to be able to measure the lateralized readiness potential (LRP). This measure can either be calculated as the difference between the EEG signal over contralateral and ipsilateral motor cortex (we used the C3 and C4 electrodes), averaged over response hands; or as the difference between (C4 – C3) for both response hands. The only difference is the factor ½ for the averaging method compared to the subtraction method; both methods result in a reflection of lateralization due to motor preparation in which hemispheric differences are averaged out.

We used three conditions: a pure rhyme condition with only trials of the rhyme task, a pure visual conditions with only trials of the visual task and a switch condition, where the two tasks had to be performed according to a fixed pattern (see below). At the beginning of the experiment subjects were instructed on paper and were able to practice the three conditions. They were told to respond as quickly as possible while keeping the amount of errors to a maximum of two or three per block. A short version of the instruction appeared on the screen at the beginning of each block, which remained until a response was given. The participants could, if they needed, take a short break during this instruction.

In the switch condition, the cell the stimuli appeared in cued the task. Because of the clockwise rotation, the task of the next trial was always predictable. Either the top two or leftmost two cells cued the one task, the remaining cells cueing the other; this leads to Monsell's (1995) AABB design (section 1.3.1).

The experiment consisted of eight sessions, each session containing ten blocks of 50 trials. The order of the blocks of a session was four switch blocks, one block of a pure condition, four switch blocks and one block of the other pure condition. After four

sessions subjects were allowed to rest and received a new instruction and training, because of the new mapping of the response keys.

### 3.3. Recordings

The EEG was recorded at a sampling rate of 250 Hz from 61 electrodes referenced to an average of both ears, linked online without electrically connecting the electrodes. The electrodes were placed according to the international 10-20 system and the electrode impedances were kept below 2 kΩ. Vertical and horizontal eye movements were recorded and used to correct the EEG electrodes for eye movements and blinks using ocular correction. Figure 2.1 shows the electrode positions and the groups we analysed together as a region of interest (ROI) to simplify the data and to keep statistical power relatively high. The amplitude and phase values of the electrodes within in a group were averaged for the ROI values used in the analyses.

### 3.4. Data analysis

In the analysis we used the RTs of the shortest and longest RSI to determine the fit of the mixture model and we only used the trials of the longest RSI for the calculation of the physiological data. Incorrect trials and trials following an incorrect trial were rejected from analysis. Also excluded from analysis were the first four trials of each

*Figure 2.1. Electrode placement and grouping*

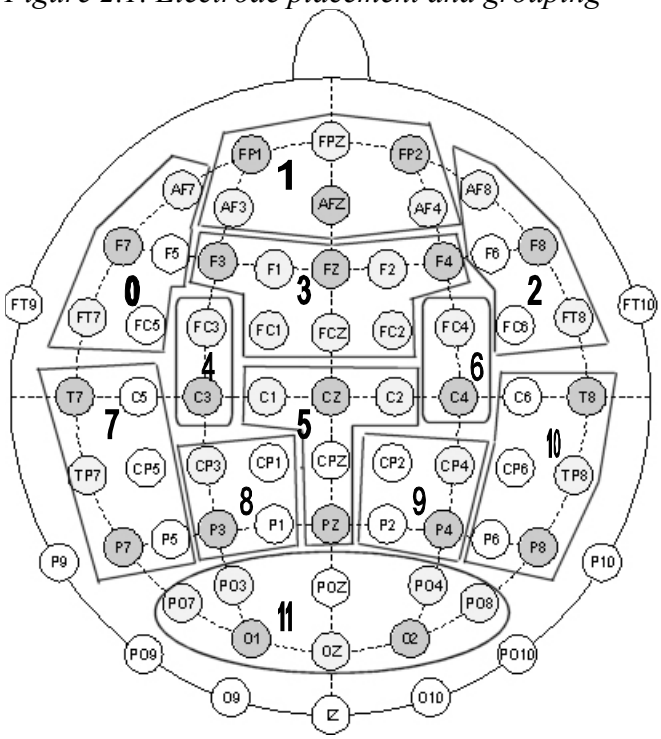


*The 12 ROI's we used were composed as follows:*

*0. FT7, F7, AF7, F5, FC5*
*1. FP1, FPZ, FP2, AF3, AFZ, AF4*
*2. FT8, F8, AF8, FC6, F6*
*3. F3, F1, FZ, F2, F4, FC1, FCZ, FC2*
*4. FC3, C3*
*5. C1, CZ, C2, CPZ, PZ*
*6. C4, FC4*
*7. T7, TP7, P7, C5, CP5, P5*
*8. CP3, CP1, P3, P1*
*9. CP4, CP2, P4, P2*
*10. T8, TP8, P8, C6, CP6, P6*
*11. PO7, PO3, POZ, PO4, PO8, O1, OZ, O2*

block and trials faster than 200 ms or slower than 2000 ms.

We used Brain Vision for segmentation, artefact rejection, baseline correction and the previously discussed current source density (section 1.2.3.4). Some points must be made about the choice of baselines in this paradigm. First, there is no natural baseline in the trials in our design. At every period during the trial, the subject is performing or has very recently performed some aspect of the task and comparisons based on any

baseline may show a systematic bias between conditions. During the RSI, the subject has just responded and may be preparing for the next trial. Physiological reflections of, for example, the level of attention at the time of either activity seem quite likely to be related to the assignment of the next trial to either the prepared or non-prepared condition. The choice of a baseline in this situation is in fact the choice of a specific contrast. Second, the results of wavelet analysis do not change if some constant is added to each value within a segment, so the choice of baseline in pre-processing for wavelet analysis is irrelevant. The baselines that could be of importance to us were those of phase and amplitude, as we were interested in changes in their time course. Fortunately, the PSA method, discussed in section 2.5, is not sensitive to added constants but only to differences in the shape of time curves. The EFA method (section 2.6) is sensitive to the baseline, if that contains an especially high or low value for that ROI at that frequency. The choice to use deviation scores for phase values attenuates the possible influence of extreme values on the ranking of somewhat less extreme values.

After the operations performed by Brain Vision the data was analysed by Gamma (de Jong, 2001), a program that calculates power and the phase-locking measures PLV and QPL by complex demodulation (section 1.2.1.1). We subtracted the ERP from the trials before calculation of power and phase to select only induced components, that is, those components not locked to the response.

A program of de Jong assigned the odds of preparation to trials. Bayes' theorem was used: the odds of preparation given a reaction time RT is equal to α times the odds of a reaction time of or below RT given preparation. Recall that α is the chance of preparation provided by the mixture model. Estimates for the chances of RT or below given preparation and non-preparation are based on the long RSI, nonswitch and short RSI, switch. The odds were used to check the validity of interpreting the fastest and slowest 25 trials as being prepared and non-prepared respectively.

### 3.5. Principle spline analysis (PSA)

In PSA (Snijders, 2001), the method we used to test differences concerning the time courses of amplitude, the data are regarded as a set of curves over time, each curve consisting of measurements at a number of times (the "knots" in the discussion

below). The subjects' curves at a point in frequency and ROI or ROI-pair are associated with one statistical test, which alleviates the number-of-tests problem relative to testing each data point individually. The test provides a level of significance for differences in the time course of amplitude or phase (-locking) between conditions. The procedure is based on the calculation of the smoothed curve that explains as much variance as possible of the subjects' difference curves at once. Differences can be calculated between conditions or between a condition and its average. The smoothing procedure is based on the theory of smoothing splines, which we introduce below before describing the PSA procedure in detail.

A spline is a piecewise polynomial: a function defined on a segmented interval that is a polynomial function within each segment. The edges of the segments are called knots. Cubic splines are a type of spline fulfilling the criteria that each polynomial is of the third degree and the first two derivatives of the polynomials meeting at a knot are equal. These splines have the property of uniquely minimizing the criterion

$$\Sigma\,(y(t) - s(t))^2 + \alpha \int (s''(t))^2 dt,$$

in which the summation is over the difference curves. The first term is the deviation of the spline from the data, representing lack of fit, the second the roughness of the spline. Roughness, the area under the squared curve of the second derivative, is the deviation of the spline from a first-degree polynomial and measures the speed of change in slopes, or less formally, of wobbliness. The α is called the smoothing parameter and determines the relative importance of fit and roughness. Hence, a given set of curves has one optimal cubic spline for each possible α, where optimality is defined as minimization of the criterion above. For an α of zero, the spline interpolates the knots, and as α approaches infinity the spline approaches a straight line. Figure 2.2 provides an illustration of the effect of increasing α.

In smoothing problems in general, the α can be chosen in a data-driven fashion by cross-validation. Cross-validation of α' s is done by calculating the spline for a given α for each possible subset of N – 1 subjects and then taking the sum of the errors of the associated left-out subjects as a lack-of-fit criterion. A number of α' s must be

tested, of which the α with the smallest lack-of-fit is selected. The procedure in PSA, described next, is a little different.

*Figure 2.2. The effect of increasing α of a spline*
*The three figures show the spline calculated for a group of noisy block waves, the α increasing from 0 to 2500 to 7500 (left to right).*

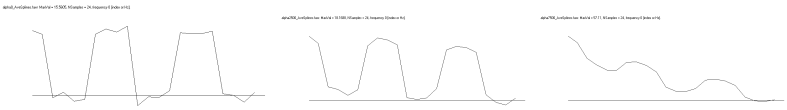

PSA is based on the principal spline (Snijders, 2001): the smoothed analogue of the principal component in factor analysis. The principal spline is the vector of weights that explains the maximum amount of variance under a roughness restriction determined by a smoothing parameter α. The α is chosen based on cross-validation using the prediction of a subject's difference curve from the principal spline based on the N – 1 other curves. Figure 2.3 shows an example of principle splines. Each plot shows a similar variability-explaining curve despite variations in the average signal. Future work will investigate further the relation of principle splines to groups of curves with certain characteristics.

Once the α-specified principal spline has been determined, the subjects are assigned spline scores: the inner product (equivalently, the weighted sum) of their difference curve with the principal spline. The spline score represents the similarity of the individual curves to the principal spline and is the measure used for determining significance.

The principal spline of difference curves describes the observed differences between the conditions. If the conditions systematically differ, the subjects will show similar difference curves, of which the principal spline will capture the major features. In this case, the subjects' spline scores will be generally large and have the same sign. If the conditions do not differ systematically, the principal spline will have only noise to explain and the subjects' overall similarity to the principal spline, and hence their spline scores, will be low and the spline scores will be randomly distributed around zero. This second consequence of the absence of an effect of condition allows

significance to be determined in a nonparametric way, via the binomial distribution of the number of positive spline scores.

*Figure 2.3. An example of a principle spline*
*The first figure shows the average difference curve between two condition, the second the principle spline explaining this difference in the sample.*

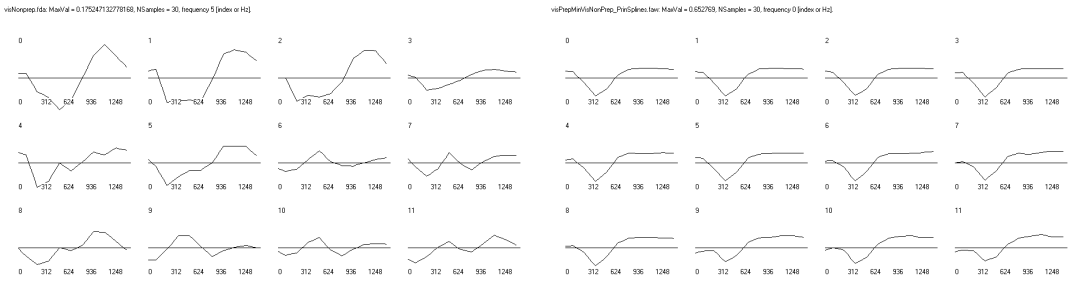

The PSA method exploits the fact that the true amplitude and phase are likely to vary in a smooth fashion over time. Hence, it seems reasonable to expect that the loss of variation due to smoothing will be more than compensated by a reduction in noise.

### 3.6. Extended Friedman Analysis (EFA)

The theory of selectivity suggests that the distribution of synchronicity over the brain could be important. That is, in some situations there is cake of synchronicity and not all brain areas can eat it, as the selectivity function would then be lost. A numerical representation wherein this win-lose / closed-game situation is expressed is the vector of rankings of PLV / QPL values over ROI-pairs at a given frequency and time: the synchronicity ranking. Snijders (2001, personal communications) helped us to specify what we term the Extended Friedman Analysis (EFA) to detect, first, points in time – frequency space at which the synchronicity ranking was consistent over subjects, and second, specific differences between ROI pairs, from consistent time – frequency points, that were significantly different from zero. Finally, the connections involved in the significant differences are selected to provide the final synchrony pattern.

The selection of time – frequency points is done via the nonparametric Friedman test for interchangeability, in our case of the values of ROI-pairs. The testing stochastic is based on the average rank of a ROI-pair over subjects. Two post-hoc tests can be used

to determine the significance of differences between ROI-pairs, of which one is $\chi^2$-distributed and the other Q-distributed. The second test is more powerful, but at this time only the first has been implemented. The final step extracts single ROI-pairs from the significant differences. Significant relations between ROI-pairs were coded as 1 (higher-than) and -1 (lower-than). Each ROI-pair was assigned the sum of its significant relations to other ROI-pairs. The total pattern of these summed significant relations are the final result, which we interpret to be significant at the level of the differences as they are directly determined from the results of the second step.

# 4. Results

## 4.1. Behavioral data

One subject's data was lost to due to a corrupted data file. RSI had a significant effect on reaction time ($F = 5.4$ (2, 9), $p = 0.029$). Reaction times for an RSI of 100 ms were significantly slower than for RSI's of 750 ms ($F = 11.9$ (1), $p = 0.006$); reaction times did not significantly decrease further from RSI 750 ms to RSI 1500 ms ($F = 1.256$ (1), $p = 0.289$). Our attempt to reduce reaction time differences between tasks was unsuccessful ($F = 25.8$ (1, 10), $p = 0.000$, the visual task being faster), but there was no interaction between task and RSI ($F = 2{,}3$, (2, 9), $p = 0.152$) or task and switch – non-switch ($F = 0.807$ (2, 10), $p = 0.390$). The effect of RSI was different in the switch and non-switch conditions ($F = 5{,}7$ (2, 9), $p = 0{,}025$). Figure 3.1 plots these results.

*Figure 3.1. Behavorial data*

*The left and right picture show the results for the rhyme and visual tasks respectively. The vertical and horizontal axes represent reaction time [ms] and RSI respectively. The RSI levels of 1, 2 and 3 represent 100, 750 and 1500 ms respectively. Switch values of 1 and 2 refer to repetition and switch trials respectively.*

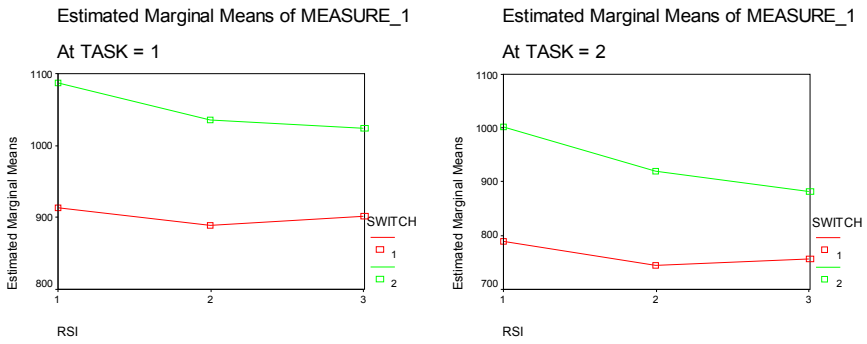


The mixture model with only the α parameter provided an acceptable fit ($G^2$ (24) = 33.23, $p = 0.0992$; this means that the lack-of-fit of the model was non-significant). Adding the δ parameter provided a significant improvement over the single-parameter model ($G^2$ (8) = 20.01, $p = 0.0103$). The estimate of δ was significantly different from zero ($\delta = 14.4$, $t = 1.97$ (10), $p < 0.05$). This suggests that subjects could not completely prepare for tasks. The odds of preparation for the fastest and slowest 25

trials were 78.6 and 19.5, respectively. Two subjects were dropped because their slowest and fastest trials were too alike in their odds of preparation.

### 4.2. ERP / LRP data

Due to equipment failures, four subjects' physiological measurements were lost completely and the EEG signals of all subjects were not properly event-locked. We used the N2 component to shift the signals to approximate their correct position relative to markers. Obviously, the data cannot be taken very seriously. The following sections are therefore restricted to the prepared – non-prepared conditions and contrast. We will discuss the prepared – non-prepared contrast in section 3.6; for now, we note that it is a complex measure, as the non-prepared condition is not neutral but may reflect the previous, unchanged task set. Figures 3.2 A and B show the ERP's and figures 3.2. E and D show the LRP's, separated by task. The prepared condition is represented in black and the non-prepared condition in red. Positive values are plotted upwards and the range is from 10 μV to -10 μV. The plots contain the data points from 2250 ms before till 650 ms after stimulus presentation, which is marked by a dashed line. Baseline correction for the ERP's was based on the first 100 ms after response (-1500 to -1400 ms). The LRP's are presented as deviation scores. All the signals were low-pass filtered, with a cut-off frequency of 15 Hz.

*Figure 3.2. ERP and LRP results*

*A. ERP, visual, rhyme = left.*

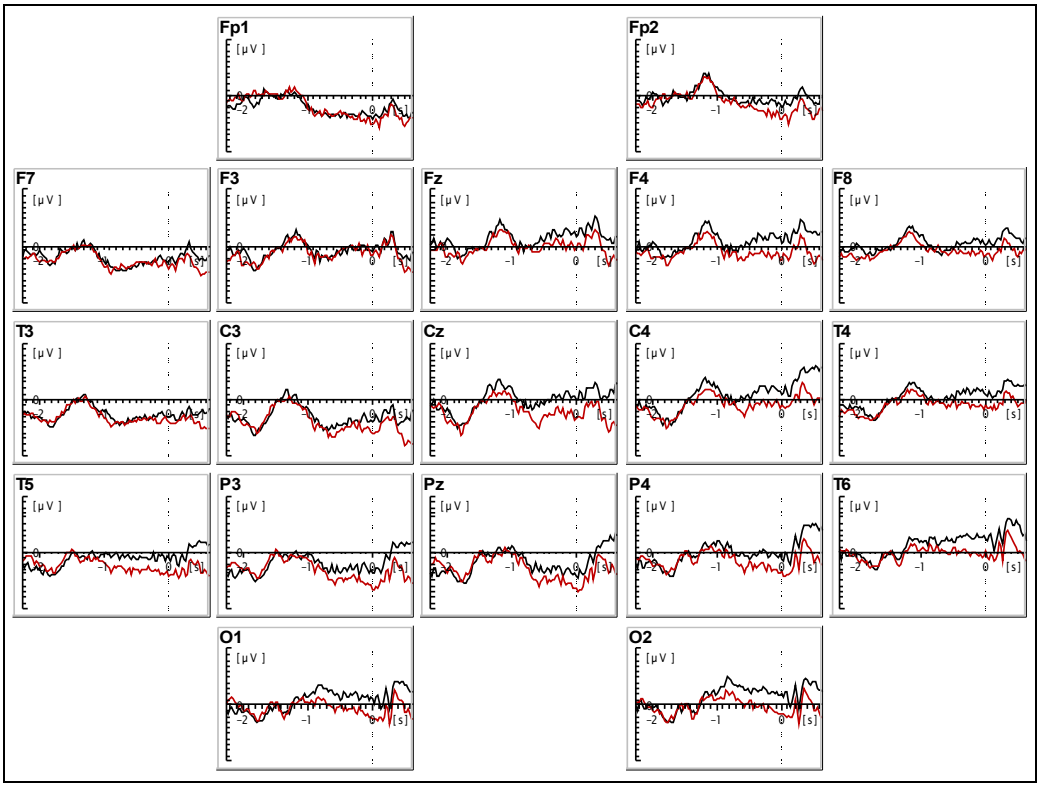


*B. ERP, visual, rhyme = right.*

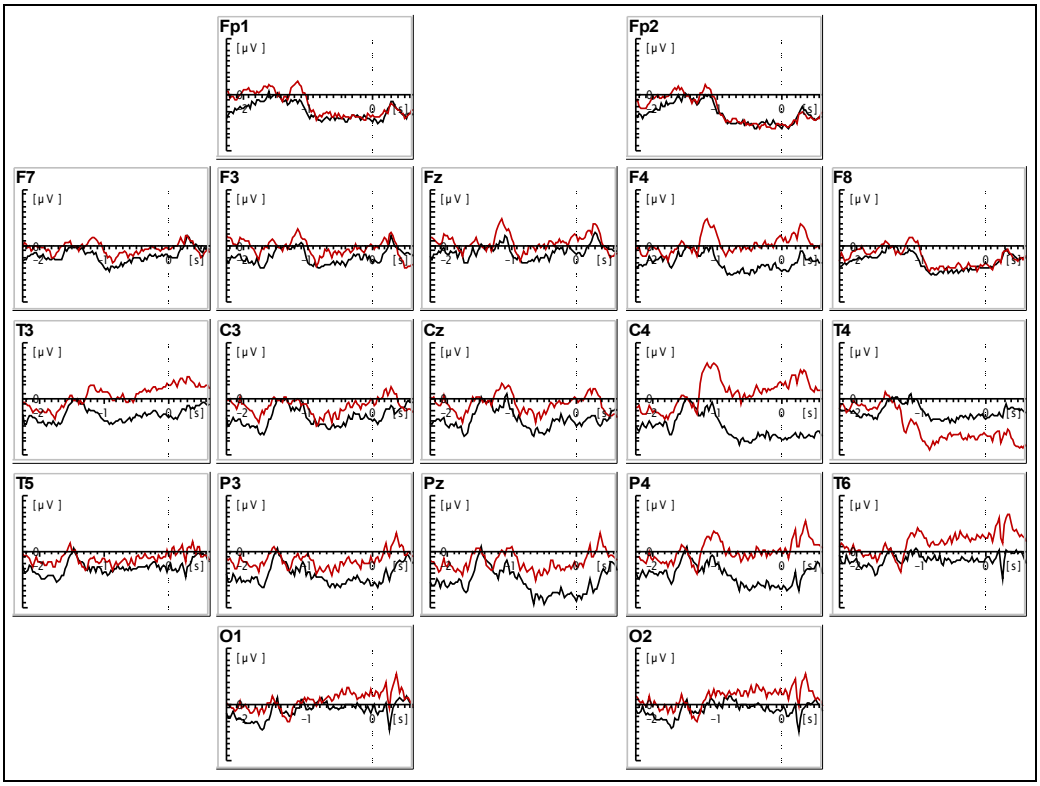

*C. Rhyme, rhyme = left.*

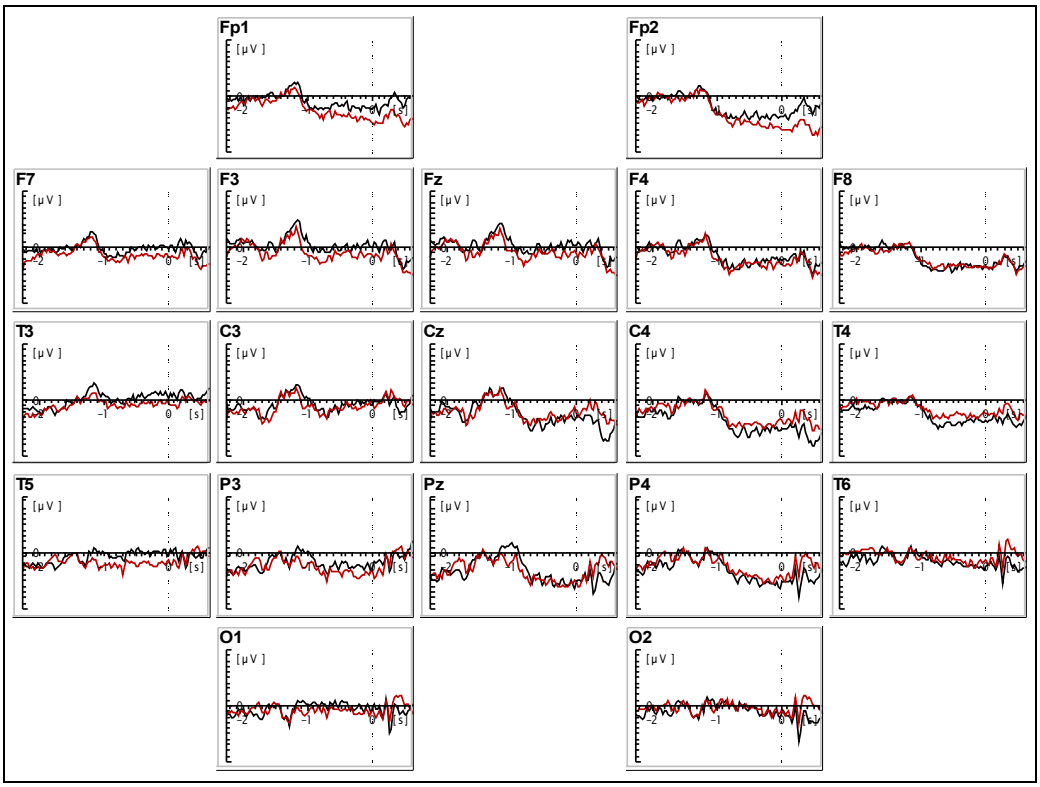


*D. Rhyme, rhyme = right.*

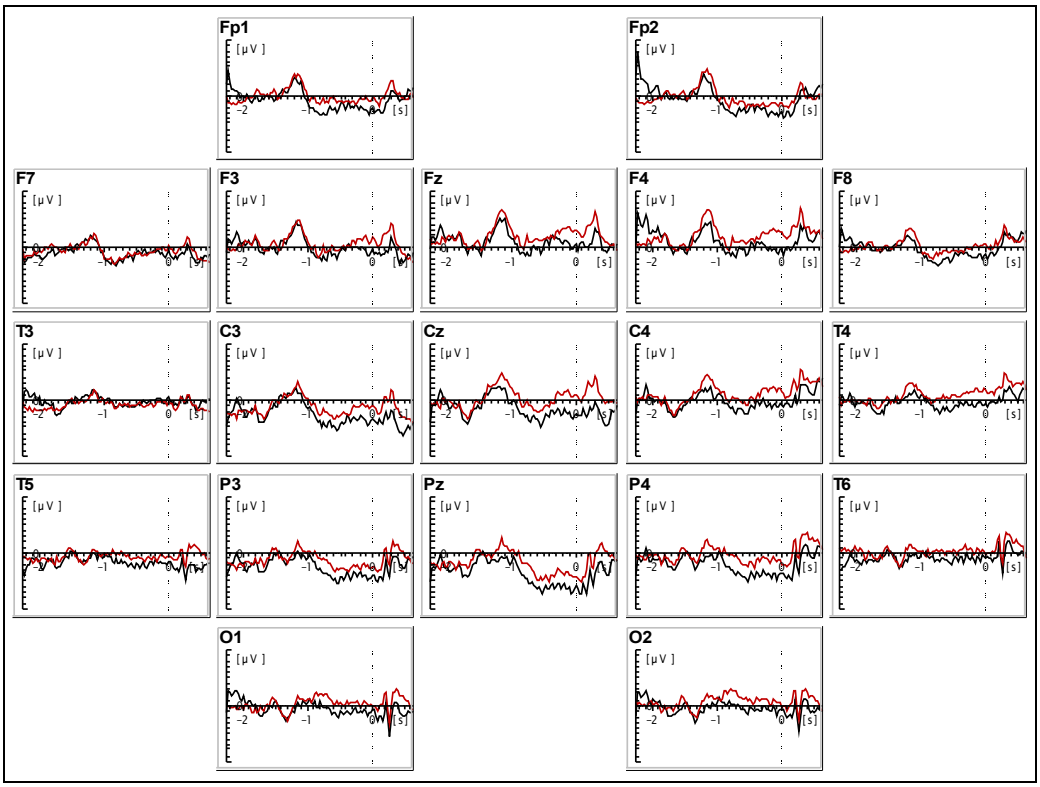

*E. LRP Visual*

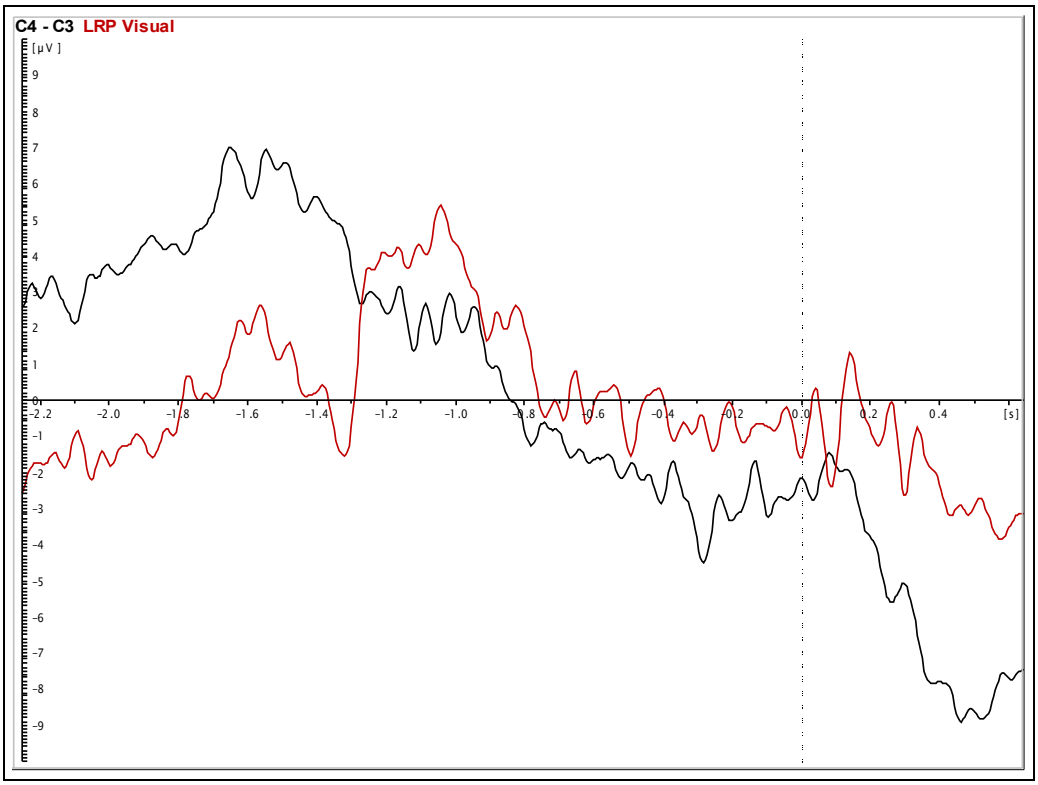


*F. LRP Rhyme*

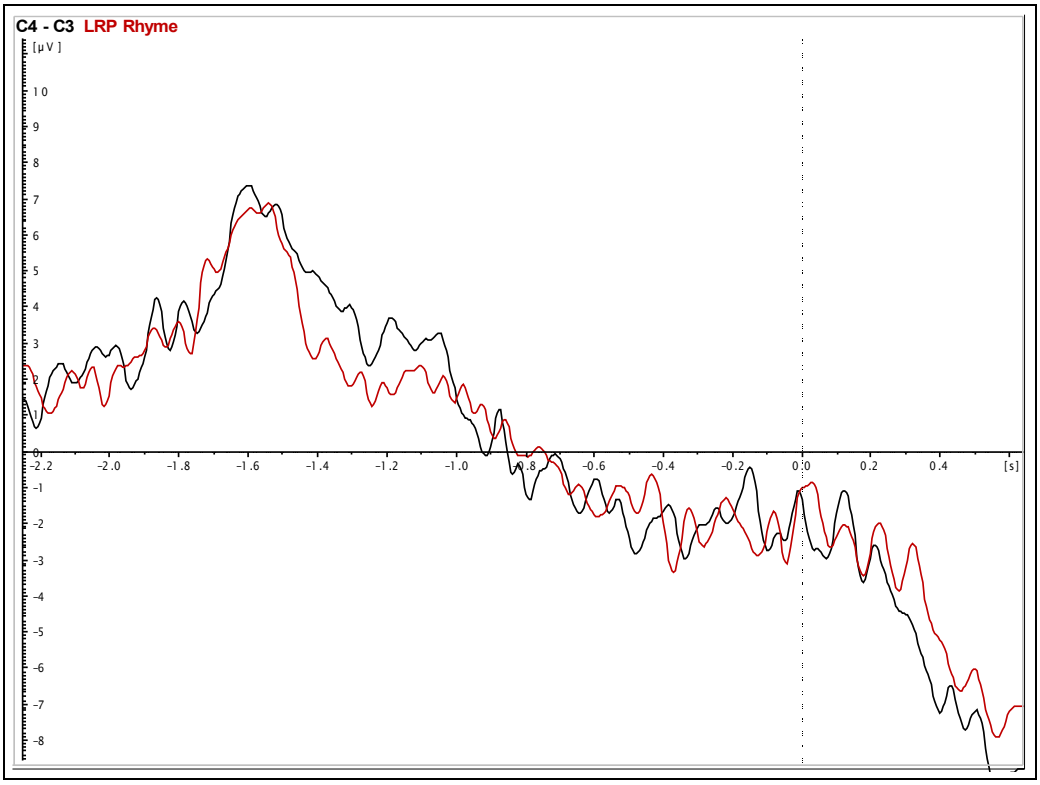

In the explanatory framework provided by the theories and results discussed in the introduction, the ERP is an inherently confounded measure, summating the activity of frequency bands with completely different functional interpretations. Even so, visual inspection of the ERP results shows a distinction between the prepared and non-prepared conditions. The ERP for the prepared condition has a larger contrast between the more positive values soon after the response and the more negative values during the pre-stimulus period than the non-prepared ERP. This preparation effect was present at most electrode sites, excepting left anterior electrodes, and is similar to the negative deflection found by Lorist et al. (2000) during the RSI preceding switch trials in comparison to repetition trials. This suggests that this difference between repetition and switch ERP's is due to the prepared trials within the switch condition.

The LRP data for the visual task show that the prepared – non-prepared states predicted by the mixture model are associated with a distinct and interpretable physiological difference during the RSI. Recall that in a given block, each task was assigned to either the left or the right hand. Part of switching tasks is therefore switching hands. Because either possible response to a stimulus on a specific trial is mapped to the same hand, subjects know with which hand they must respond on the next trial; this depends on the position of the trial in the AABB sequence, not on the as yet unknown stimulus. During a repetition RSI, motor attention is already focussed on the correct hand for the next trial; that is, the response set concerning the keys for that hand will have been activated as part of a completed task-set reconfiguration. Responses on switch trials require that motor attention must shift to the previously unused hand. The theories in section 1.3 concerning preparation suggest that this shift, or change in activated response-representations, may occur prior to stimulus presentation. In this case, the same stimulus must be re-mapped to different response keys. Due to our choice of response keys and the change in task - hand mapping halfway through the experiment, we were able to use the LRP as a measure for task-set reconfiguration.

The LRP results for the visual condition suggest that when the odds of preparation provided by the mixture model are high for a given trial, subjects had switched to the new task-set prior to stimulus presentation. In contrast, the rhythm data do not show differences in the LRP due to preparation. Other measures to be discussed below also indicate a difference in the kind of preparation that takes place for the two kinds of tasks. Perhaps the relative benefit of pre-activating the response hand is lower in the more complex rhyme task, leading the LRP to be relatively independent of preparation for this task.

### 4.3. Amplitude data

Figures 3.3.2 and 3.3.3 show a selection some of the more interesting amplitude time courses that were marked as significant by the PSA method (figure 3.3.1). The 12 subplots contain the data for the ROI's. The numbering of ROI's is provided in the Method section (figure 2.1). The horizontal and vertical axes of each subplot represent time in ms and frequency respectively. The mapping of values on the vertical axis to frequency means is given in figure 3.3.1. Amplitude is color coded, the specific coding being given in the color bar over each plot. We expected the results for the different response hands to be similar, but this was not the case. Six subjects are very likely not to be sufficient for PSA to provide reliable results The level of significance was the highest achievable with the number of subjects we could eventually use: 0,016. Given the amount of tests used, obviously this does not control for overall alpha. The time courses in figures 3.3.2 and 3.3.3 reveal three kinds of differences picked up by PSA. In 3.3.2 A (rhyme task), the 5 Hz prepared amplitude curve over visual cortex crosses over the non-prepared curve: up to 650 msec post-response the amplitude is lower for preparation, from 650 msec onwards the preparation curve lies above that for non-preparation. Figure 3.3.2. B (rhyme task) shows a relative decrease of 10 Hz amplitude around 900 msec post response over regions in the left hemisphere during preparation. Figure 3.3.3 A (visual task) shows a sharp 42 Hz peak at 650 msec over left and dorsal anterior regions. It is suggestive that this is the same time as the increase of delta activity at irrelevant areas found for the rhyme task.

*Figure 3.3.1. Time courses marked as significant by PSA*

*The values on the vertical axis represent frequency means as follows. The standard deviations in frequency of each band were 1 Hz for 5 Hz, 2 Hz for 10 and 12 Hz, and 3 Hz for all following frequency bands.*

*1: 5 Hz* *2: 10 Hz* *3: 12 Hz* *4: 15 Hz* *5: 18 Hz* *6: 21 Hz*

*7: 24 Hz* *8: 27 Hz* *9: 30 Hz* *10: 33 Hz* *11: 36 Hz* *12: 39 Hz*

*13: 42 Hz*

*A. Visual prepared – visual non-prepared, rhyme = left*

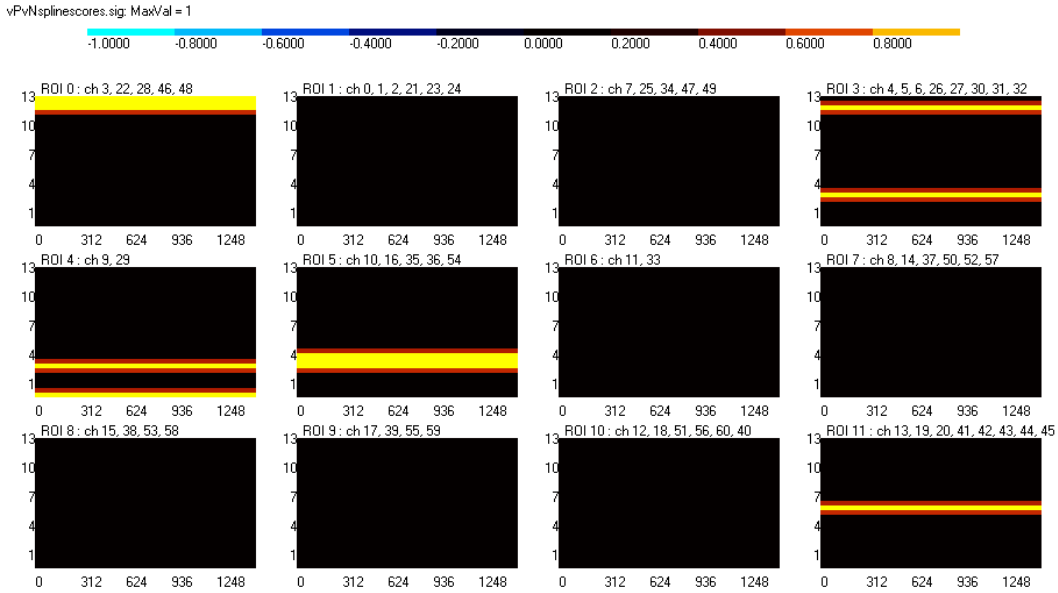


*B. Visual prepared – visual non-prepared, rhyme = right*

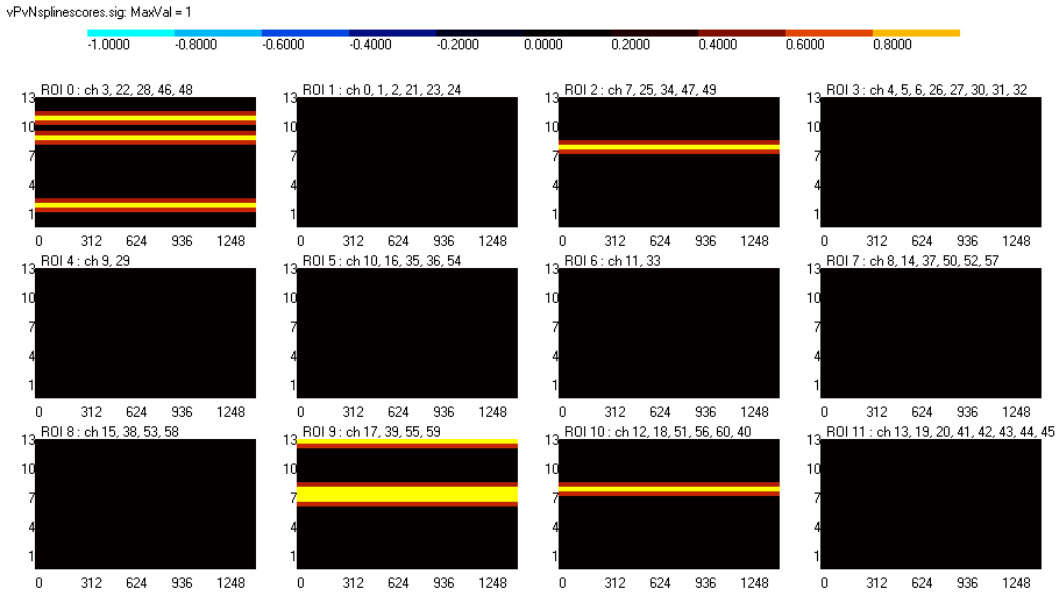

*C. Rhyme prepared – rhyme non-prepared, rhyme = left*

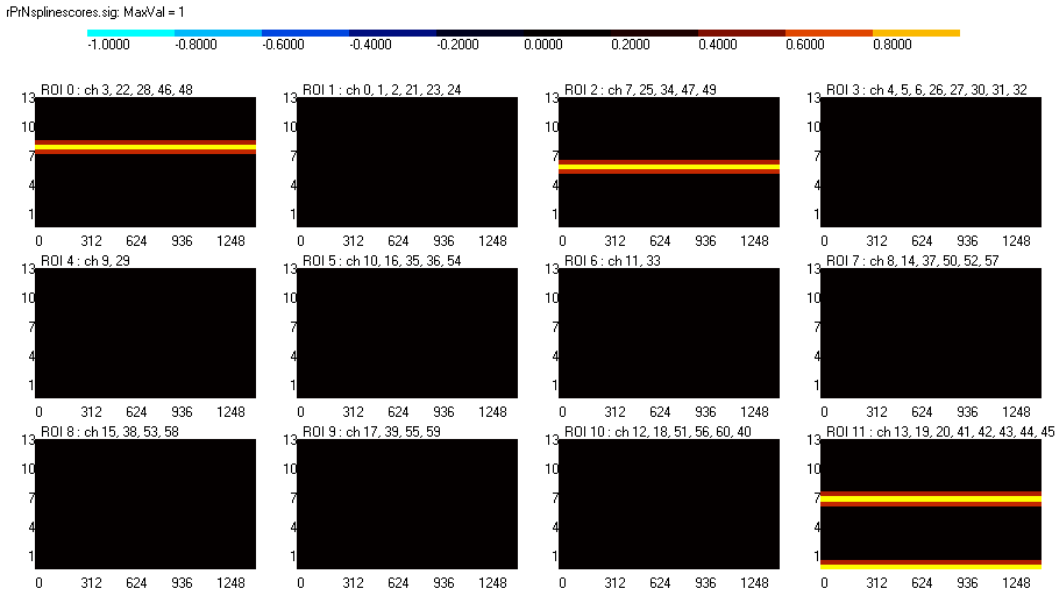


*D. Rhyme prepared – rhyme non-prepared, rhyme = right*

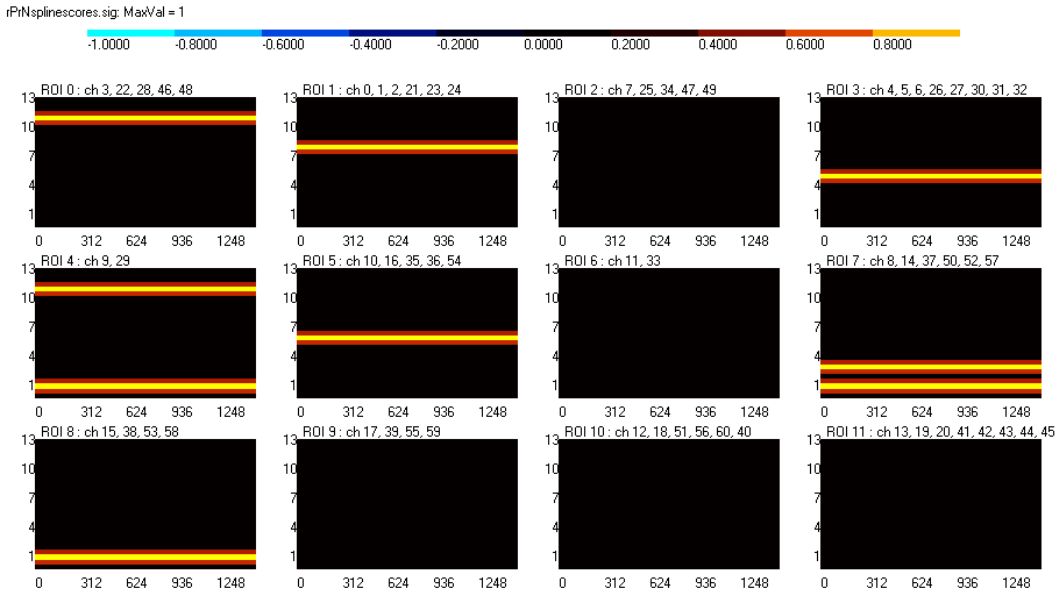

*Figure 3.3.2. Low-frequency amplitude time courses contrasting rhyme prepared – non-prepared*

*The following curves were marked as significant by PSA at an individual significance level of 0,016. The horizontal axis is time, the vertical amplitude. The vertical scale is determined by the maximum value, which covers the vertical distance between plots.*

*A. Rhyme, 5 Hz, rhyme = left*

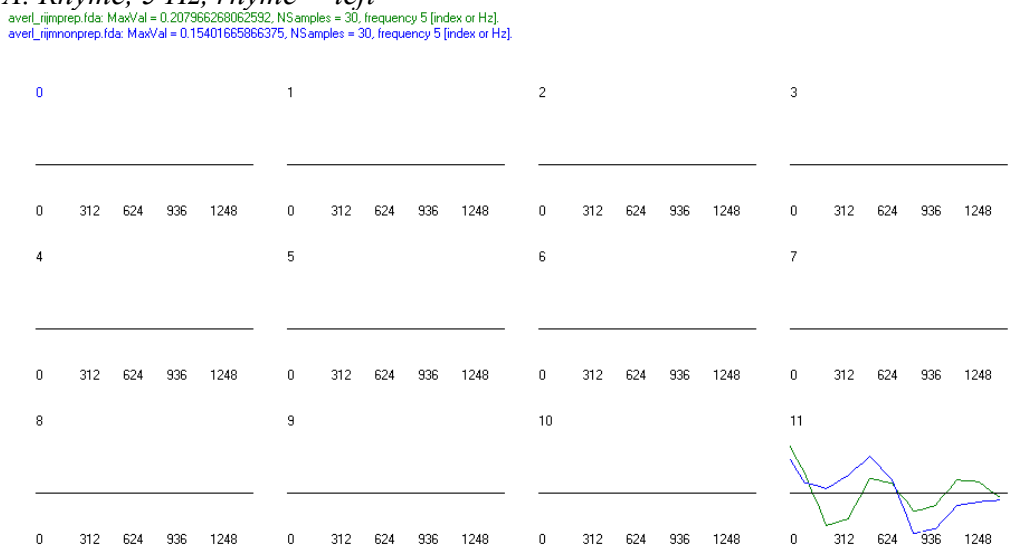


*B. Rhyme, 10 Hz, rhyme = right*

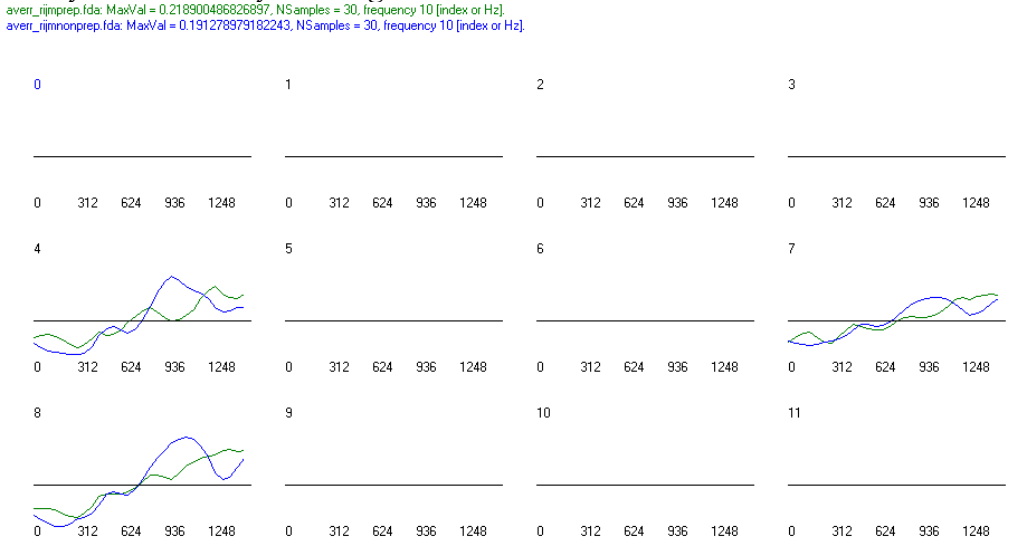

*Figure 3.3.3. Low-frequency amplitude time courses contrasting visual prepared – non-prepared*

A. Visual, 42 Hz, rhyme = left

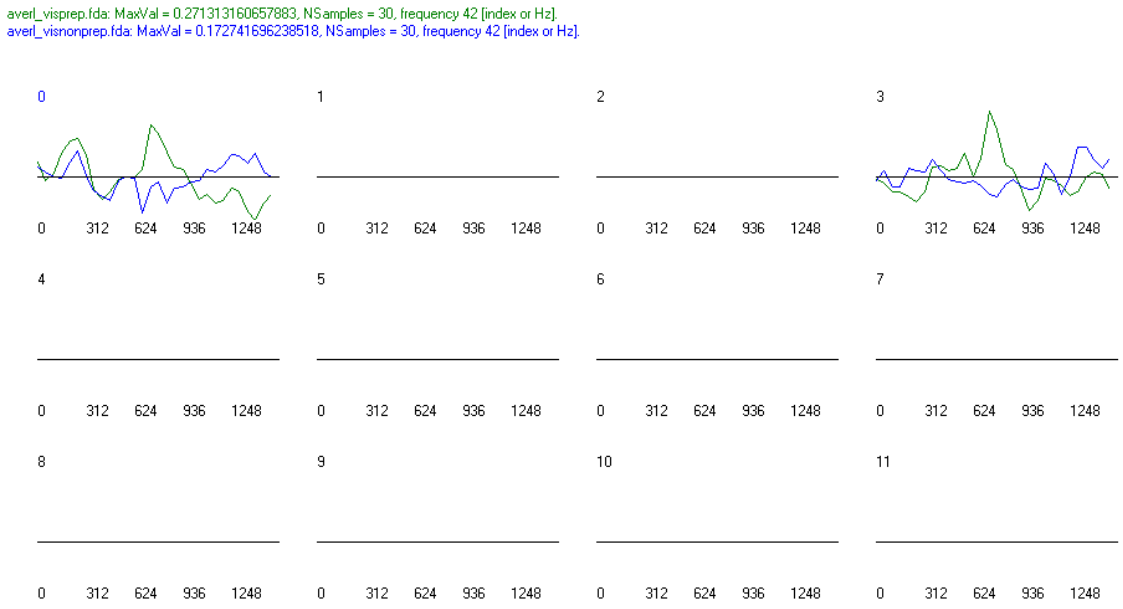


B. Visual, 12 Hz, rhyme = right

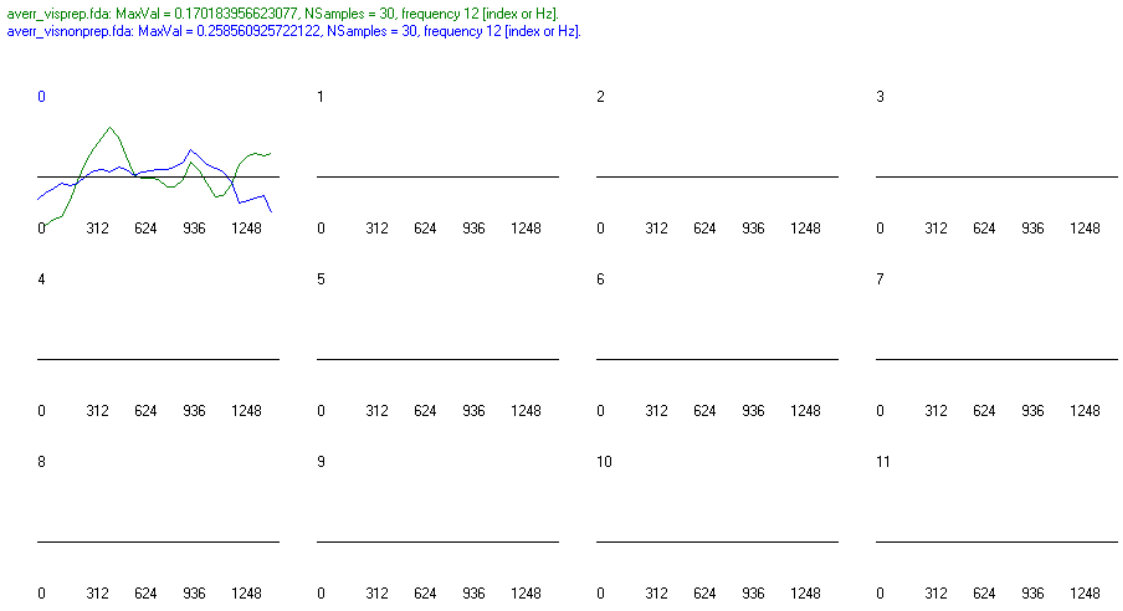

Figure 3.4 shows the complete power plots acquired by subtracting the non-prepared from the prepared data for both tasks, for both response-hands. Figure 3.5 shows the results of normalization per frequency, where the values are z-scores based on the standard deviation over the samples and regions at each frequency mean. Normalization may reveal different patterns by enhancing variability at higher frequency bands, which have lower amplitudes, to the same scale as the lower frequencies. With these data, normalization did not seem to clarify much. The most prominent effects were those identified by PSA.

*Figure 3.4. Contrasts between prepared and non-prepared conditions*

*A. Visual prepared – visual non-prepared, rhyme = left*

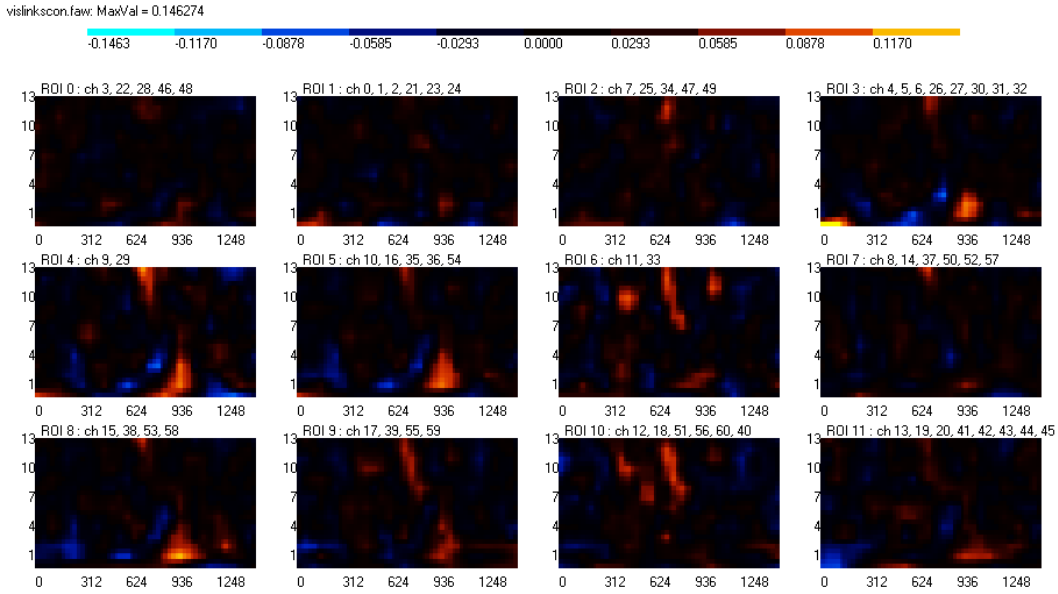


*B. Visual prepared – visual non-prepared, rhyme = right*

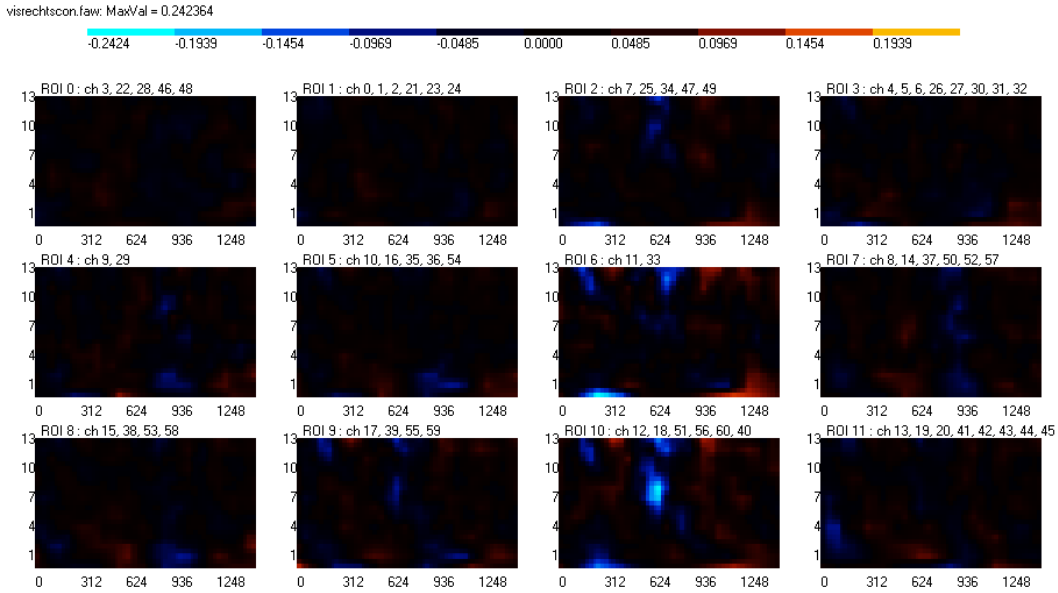

*C. Rhyme prepared – rhyme non-prepared, rhyme = left*

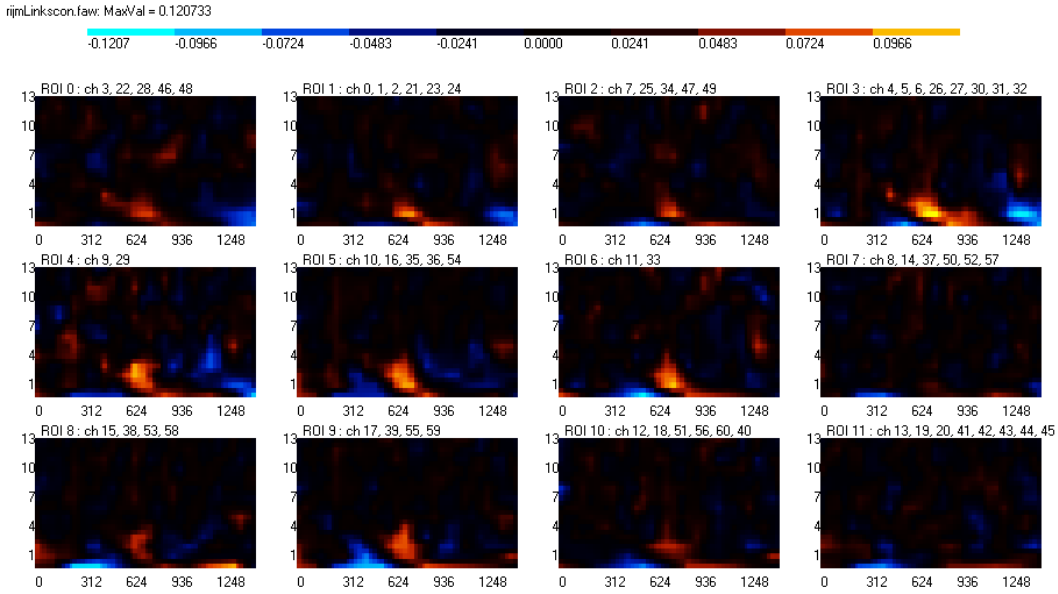


*D. Rhyme prepared – rhyme non-prepared, rhyme = right*

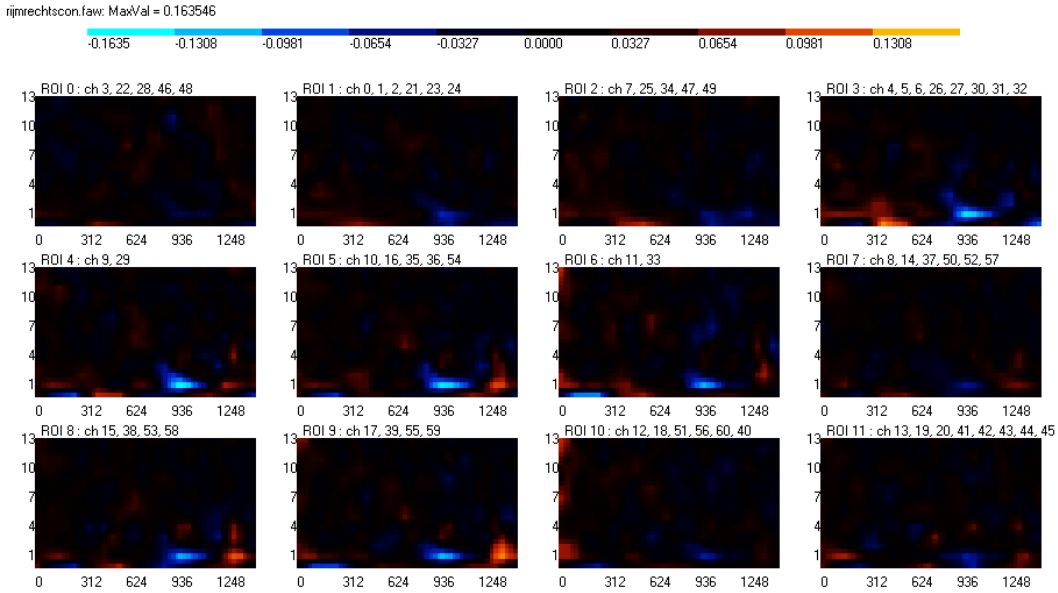

*Figure 3.5. Contrasts, normalized per frequency*

*A. Visual prepared – visual non-prepared, rhyme = left*

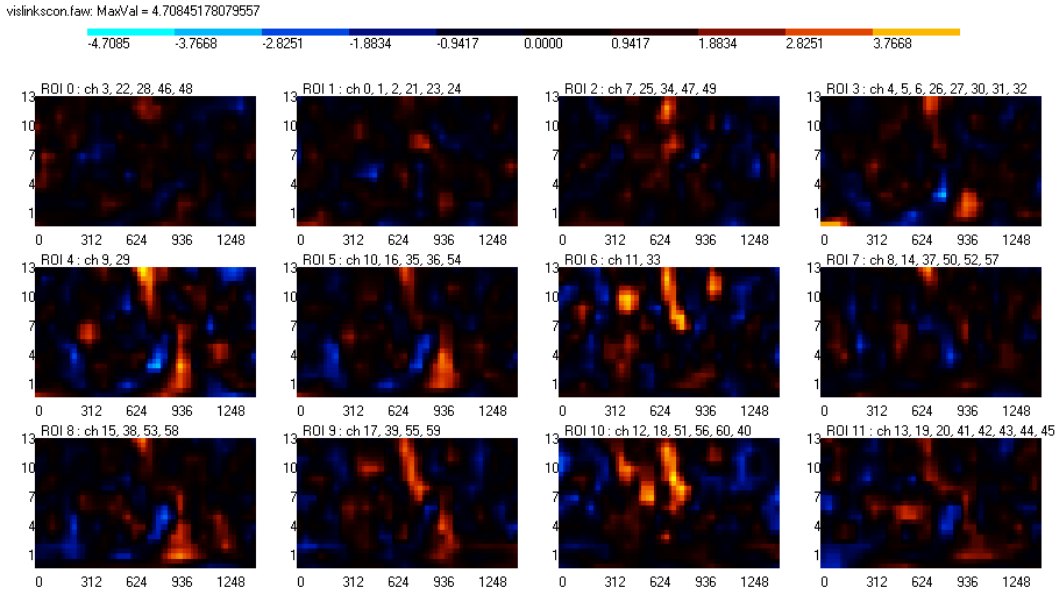


*B. Visual prepared – visual non-prepared, rhyme = right*

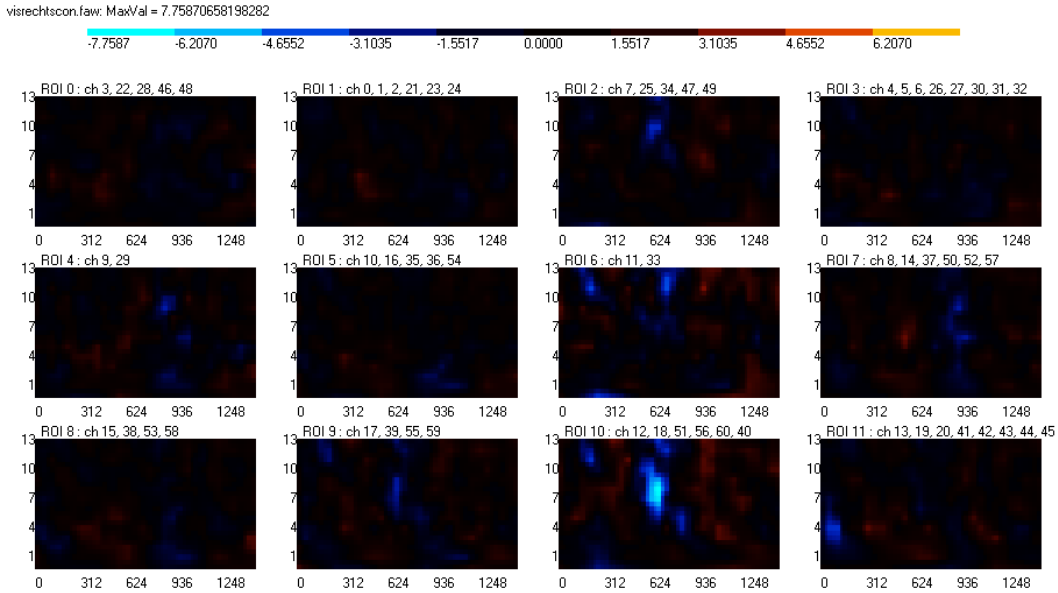

*C. Rhyme prepared – rhyme non-prepared, rhyme = left*

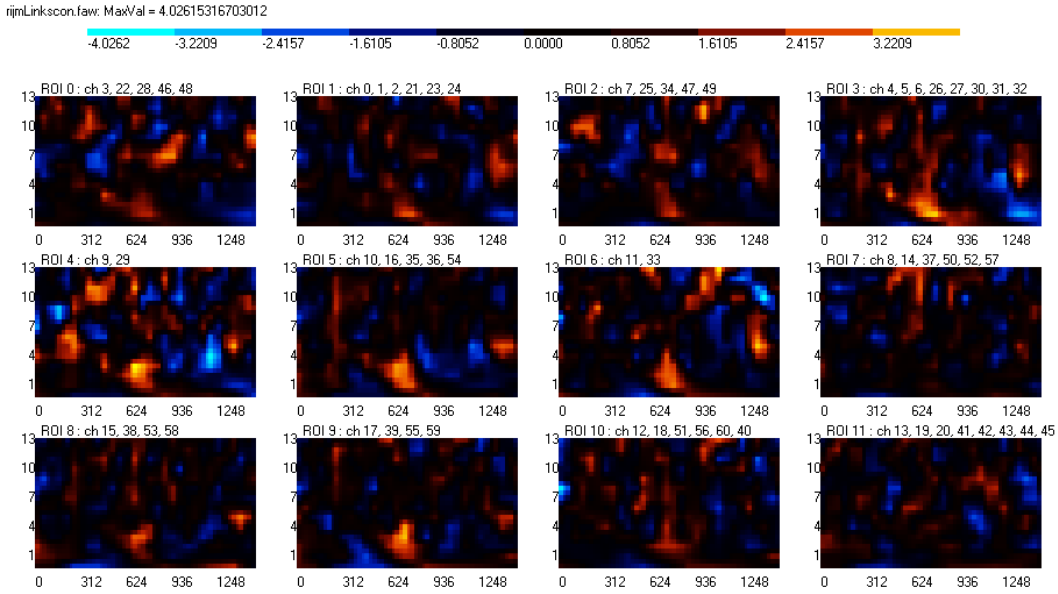


*D. Rhyme prepared – rhyme non-prepared, rhyme = right*

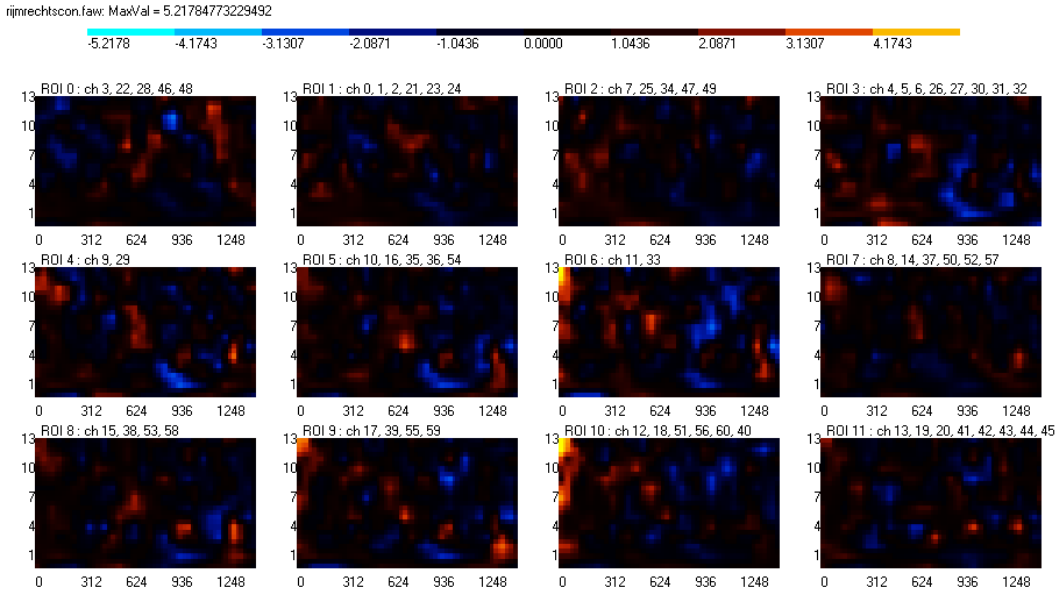


## 4.4. PLV data

The PLV data in figure 3.7 are based on a pseudo-statistical representation of the data, where z-scores are calculated based on the standard deviation of all data points, and only values above a criterion are plotted. These values represent a synchrony between two regions that are represented spatially, the point of view looking down on the head. Frontal positions are plotted at the top. Color now codes frequency (see figure 3.3.1 for the coding of frequency values to frequency means). Figure 3.8 shows the results of EFA for synchrony (positive values for the relationship coding described in section

2.6), figure 3.9 for desynchronization (negative values). The most significant results are shown as lines with an arrow indicating the time at which the significance difference occurred. The ratio of the time from the start of the RSI to the occurrence to the total period is equal to the ratio of the distance between the (arbitrary) starting point of the line and the tip of the arrow to the total length of the line. That is, an arrow on the middle of the line indicates an occurrence halfway through the RSI, one near the starting point an occurrence soon after the start of the RSI, etc. The EFA criteria were 100 and 15 for the Friedman and post-hoc procedures respectively. The post-hoc criteria with the current method could not be set to an acceptable level of significance without losing all resolution. The EFA results therefore should be seen as a display of earmarked connections, that is, the most significant connections attainable. In this and the following section the post-hoc criterion was set at a level at which the results were selective and sensitive enough for comprehensible patterns to be seen. These results should be taken as examples of the type of data that wavelet analysis provides; they are by no means intended to be seen as statistically significant.

Four trends can be seen in these data. First, for both tasks significant EFA results were almost exclusively found for the right-handed condition (only one significant connection was found when the response was left-handed). This suggests that responding with the non-dominant hand is either hard to prepare for, or requires a non-systematic kind of preparation. Second, long-range synchrony is common at all frequencies. Third, prefrontal areas were often involved in connections in the EFA patterns. Every right-handed connection was either between a prefrontal area and some other area or between two areas of which one had a significant connection to prefrontal cortex. Fourth, artefactual synchrony due to muscle activity doesn't seem to be a problem as synchronies were found at specific frequency bands.

*Figure 3.7. Pseudo-statistical representation of PLV results*

Criterion = 5.0.

*A. Visual prepared – visual non-prepared, rhyme = left*

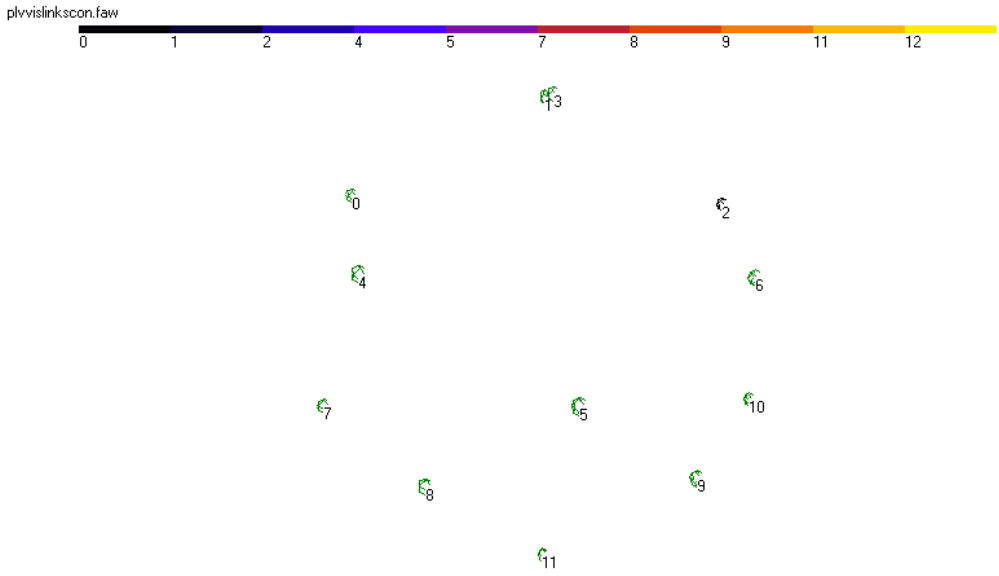


*B. Visual prepared – visual non-prepared, rhyme = right*

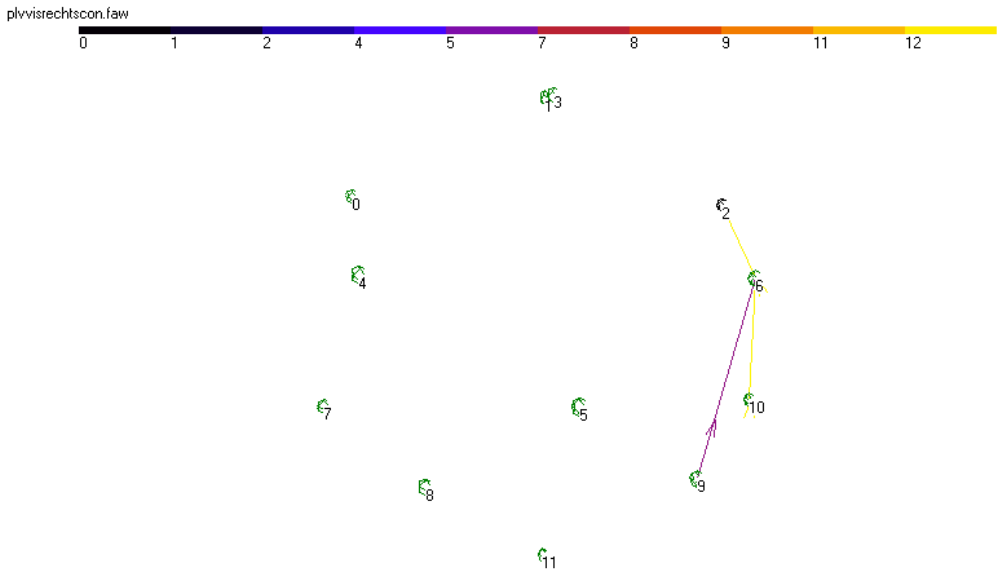

*C. Rhyme prepared – rhyme non-prepared, rhyme = left*

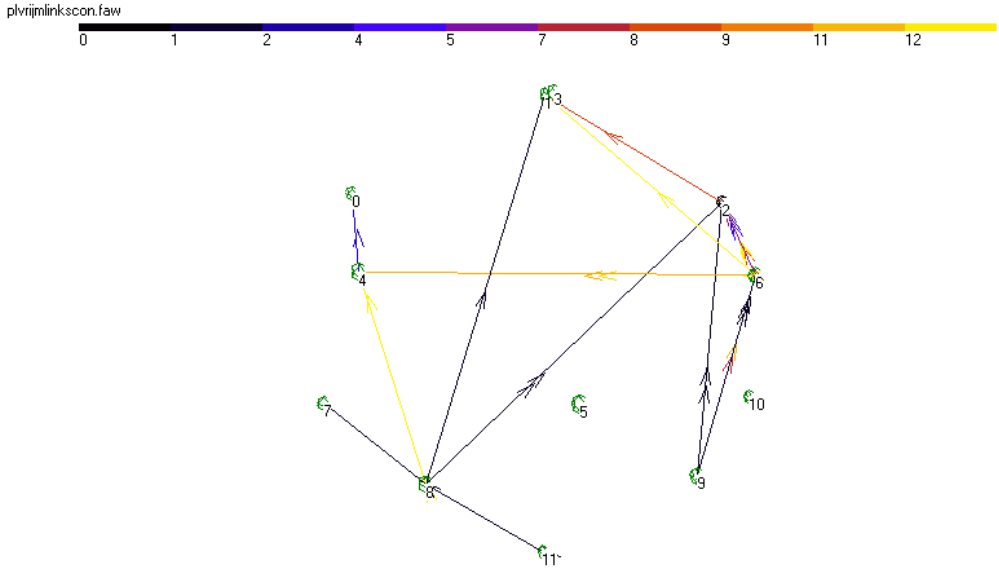


*D. Rhyme prepared – rhyme non-prepared, rhyme = right*

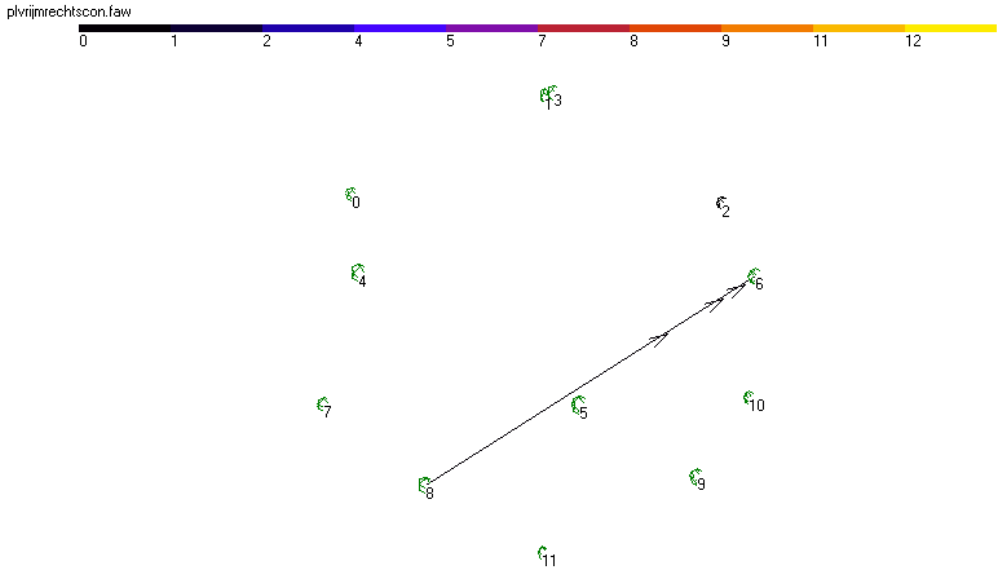

*Figure 3.8. EFA results: synchrony*

*A. Visual prepared – visual non-prepared, rhyme = left*

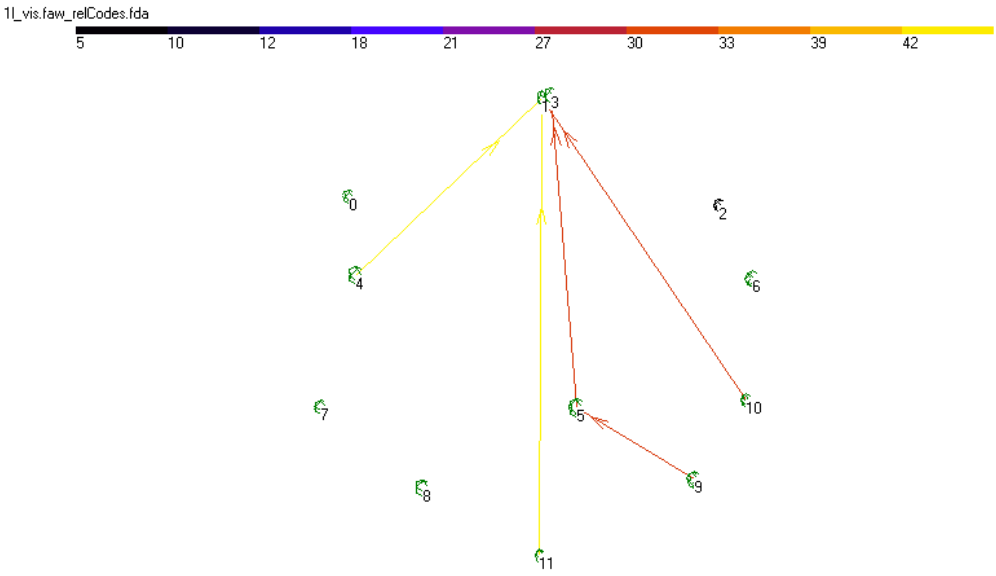


*B. Visual prepared – visual non-prepared, rhyme = right*

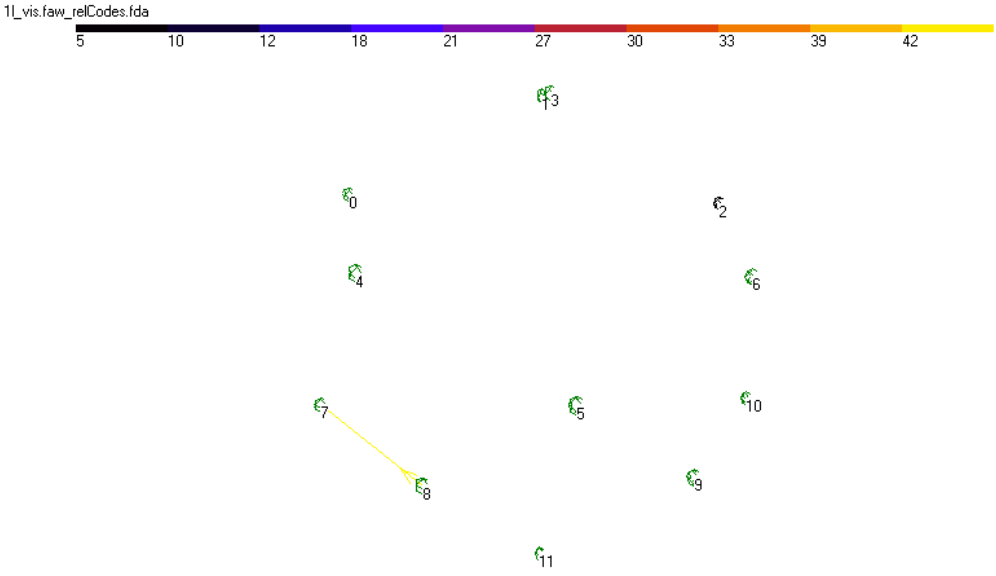

*C. Rhyme prepared – rhyme non-prepared, rhyme = left*

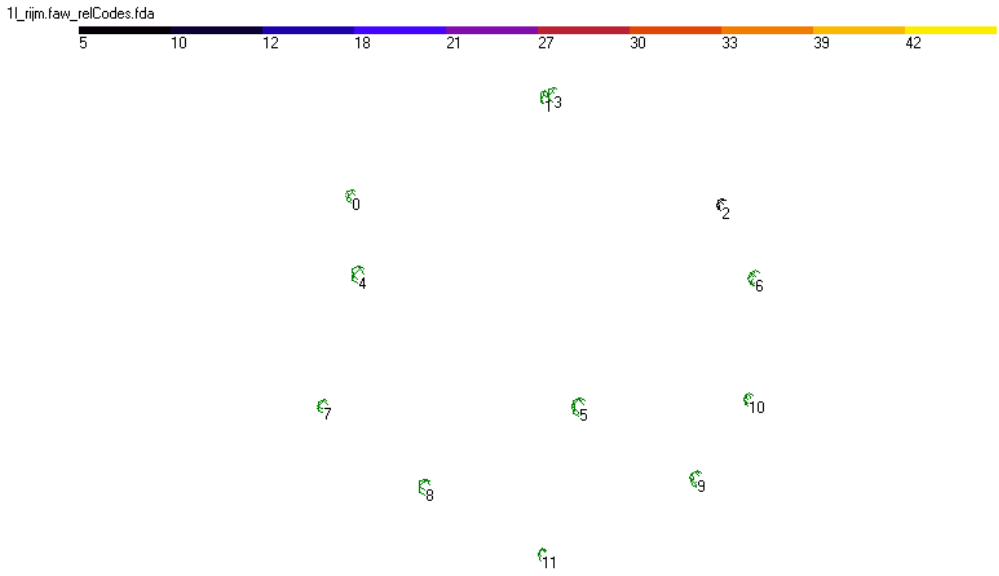


*D. Rhyme prepared – rhyme non-prepared, rhyme = right*

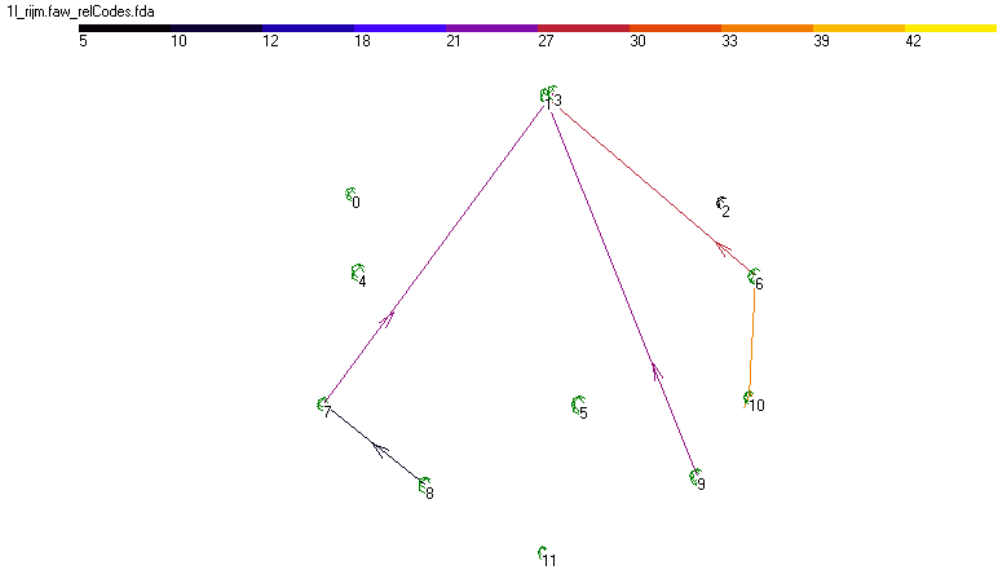

*Figure 3.9. EFA results: desynchronization*

*A. Visual prepared – visual non-prepared, rhyme = left*

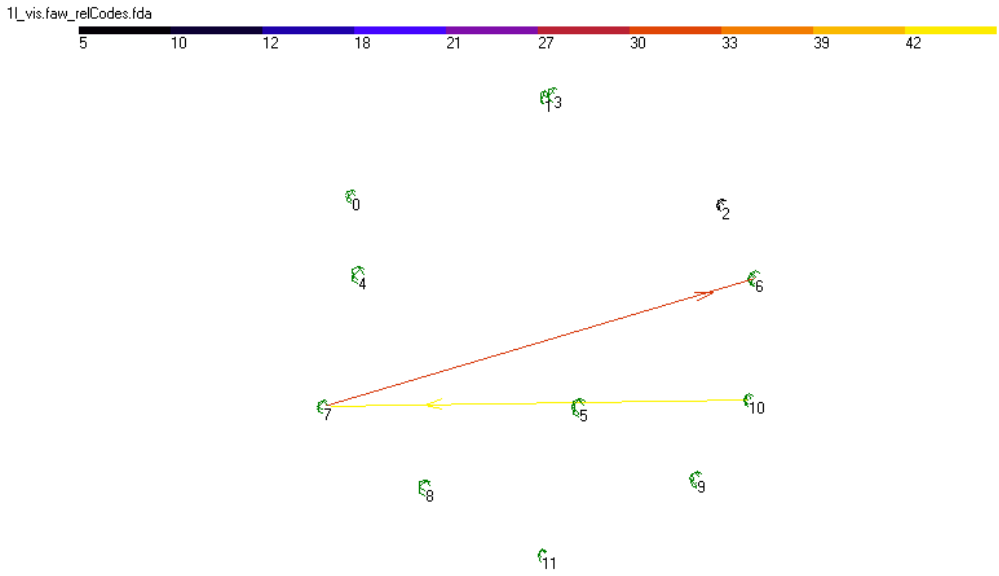


*B. Visual prepared – visual non-prepared, rhyme = right*

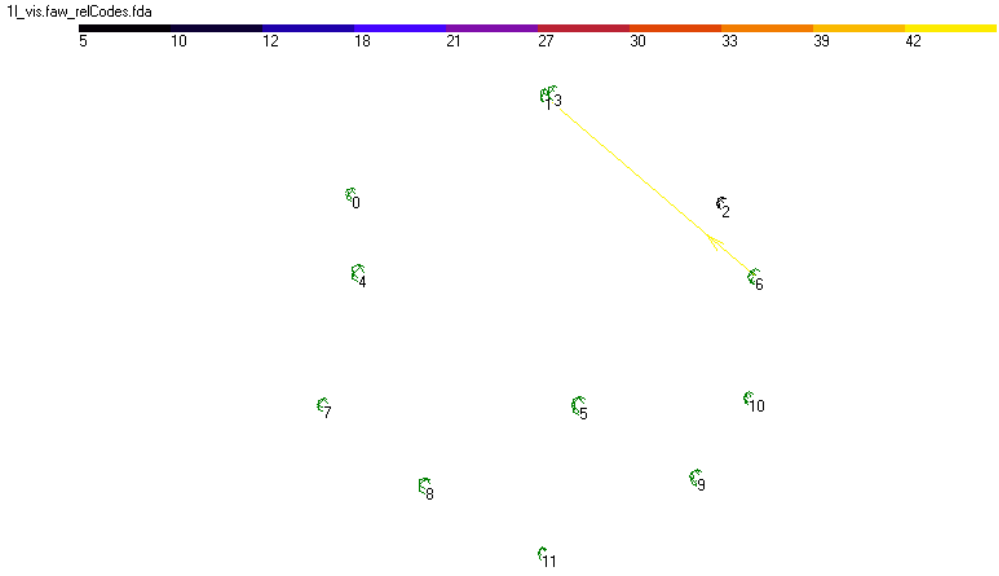

*C. Rhyme prepared – rhyme non-prepared, rhyme = left*

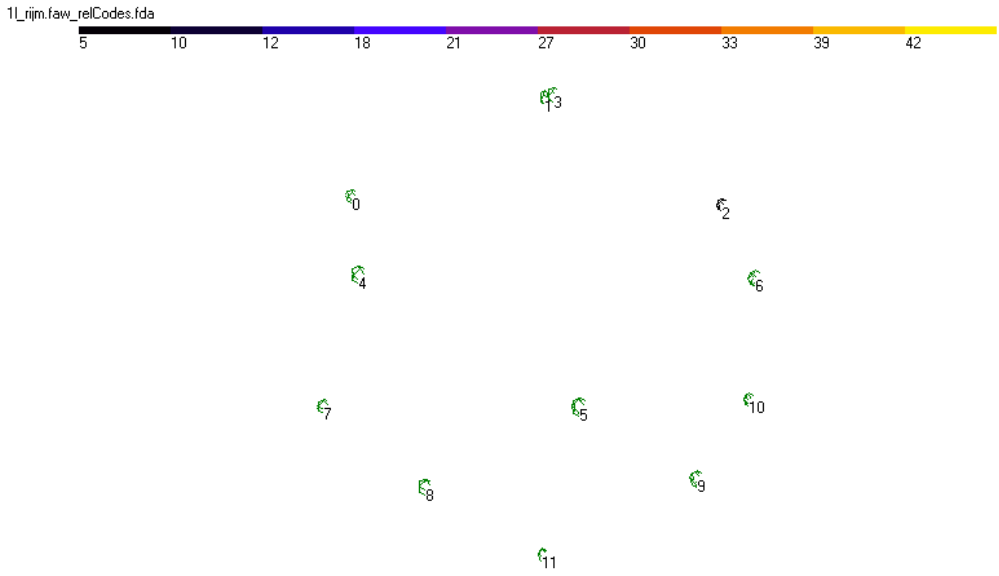


*D. Rhyme prepared – rhyme non-prepared, rhyme = right*

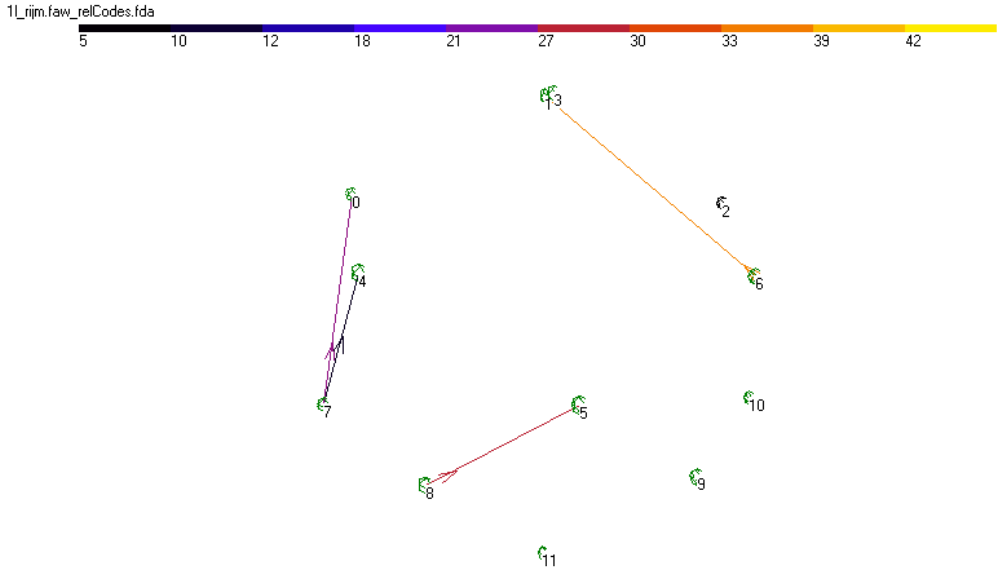


## 4.5. QPL data

The QPL data will be presented in the same fashion as the PLV data above. Note that in the pseudo-statistical representation the criterion is 4.0. No connections were

selected at 5.0. The EFA criteria were 100 and 18 for the Friedman and post-hoc procedures respectively.

In the visual condition, the pseudo-statistical contrast provides an interesting view, high level frequency occuring around prefrontal and motor areas. Almost uniquiely in these data, the different response hands showed similar and even partly mirrored patterns. The right-handed rhyme condition was also interesting but completely different. The ipsilateral motor area was involved with an alpha band synchrony, which fits well with the putative antagonistic relation of alpha coherence with local processes. The EFA results show less consistent trends than for PLV, although, again, prefrontal cortex is often involved, long-range synchronies are common and results are found for specific frequency bands. The alpha band desynchronization in the right-handed visual contrast concerned with parietal areas fits well with their putative importance in task-switching (e.g. Sohn et al., 2000).

*Figure 3.10. Pseudo-statistical representation of QPL results*

Criterion = 4.0.

*A. Visual prepared – visual non-prepared, rhyme = left*

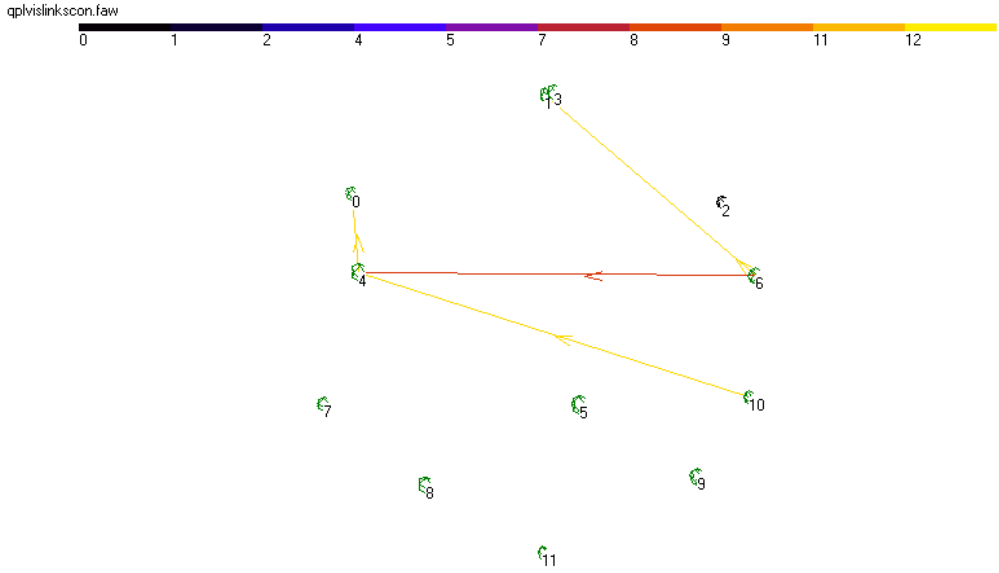


*B. Visual prepared – visual non-prepared, rhyme = right*

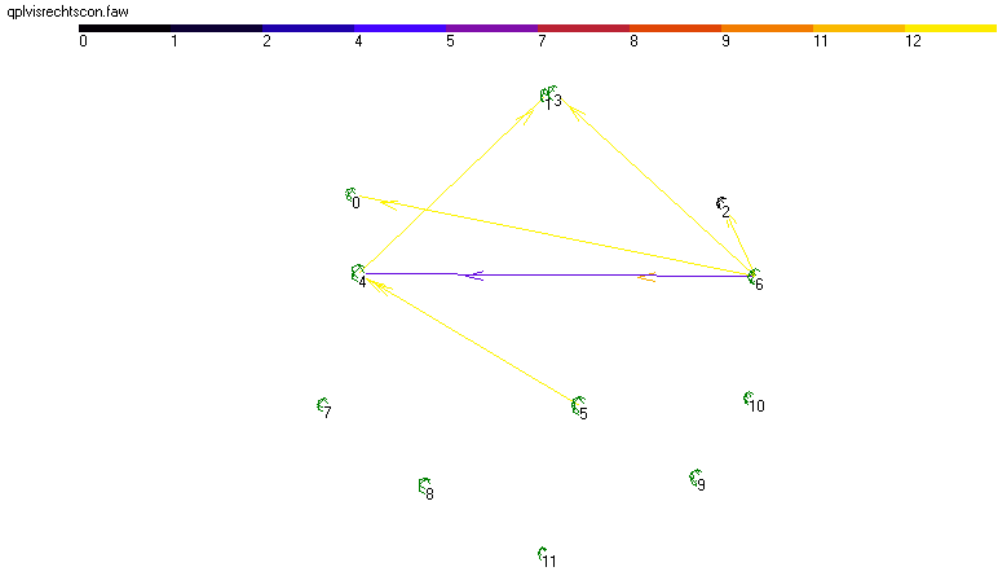

*C. Rhyme prepared – rhyme non-prepared, rhyme = left*

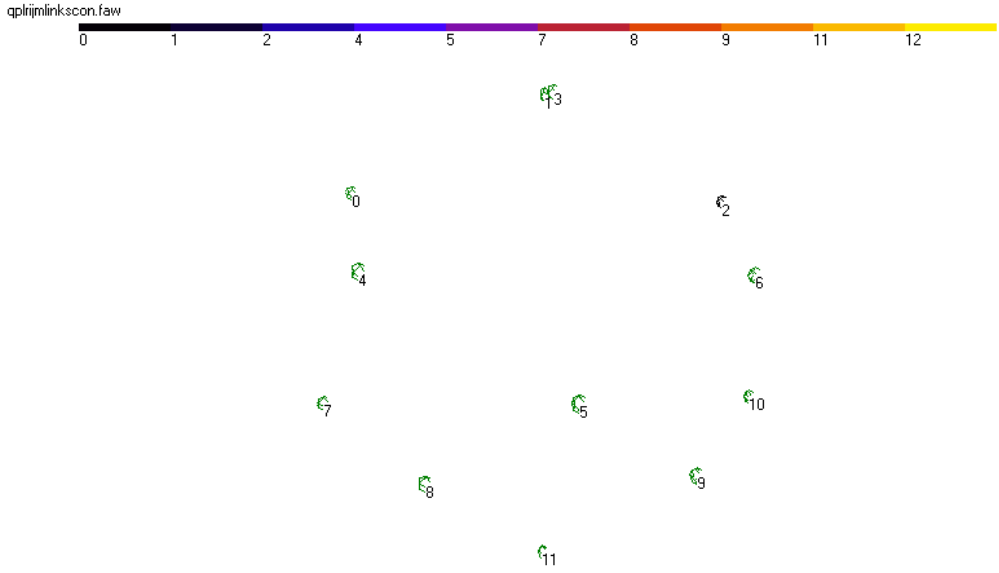


*D. Rhyme prepared – rhyme non-prepared, rhyme = right*

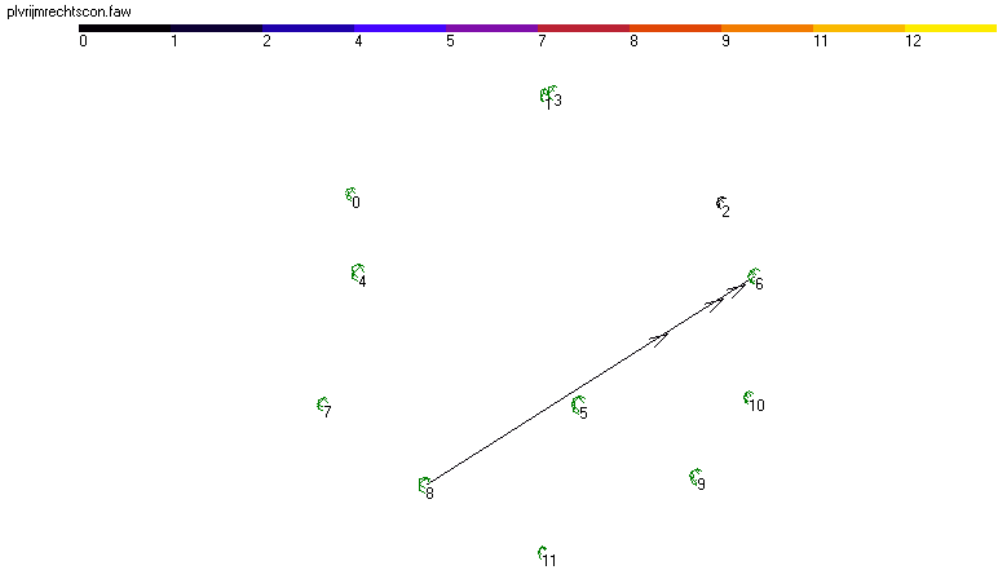

*Figure 3.11. EFA results: synchrony*

*A. Visual prepared – visual non-prepared, rhyme = left*

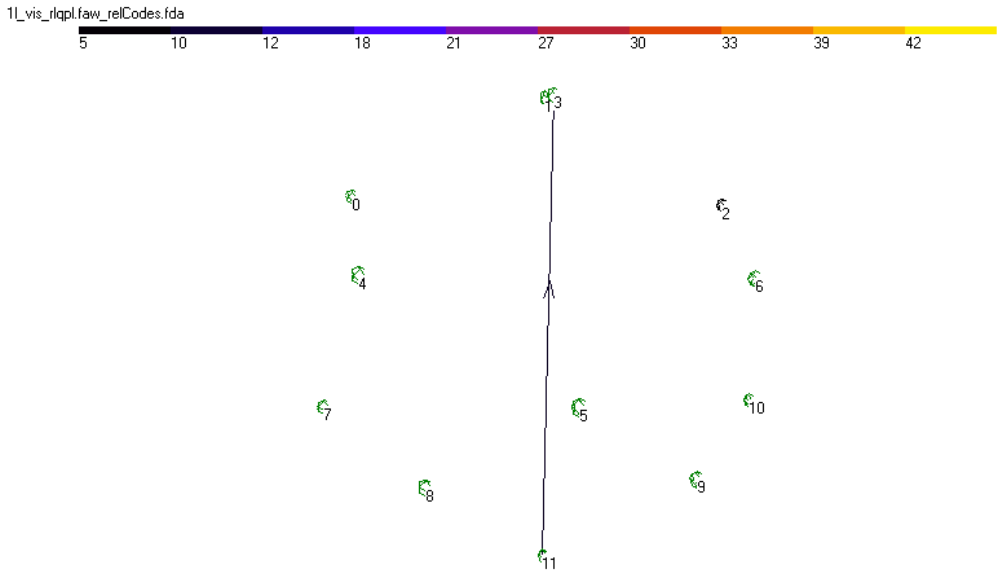


*B. Visual prepared – visual non-prepared, rhyme = right*

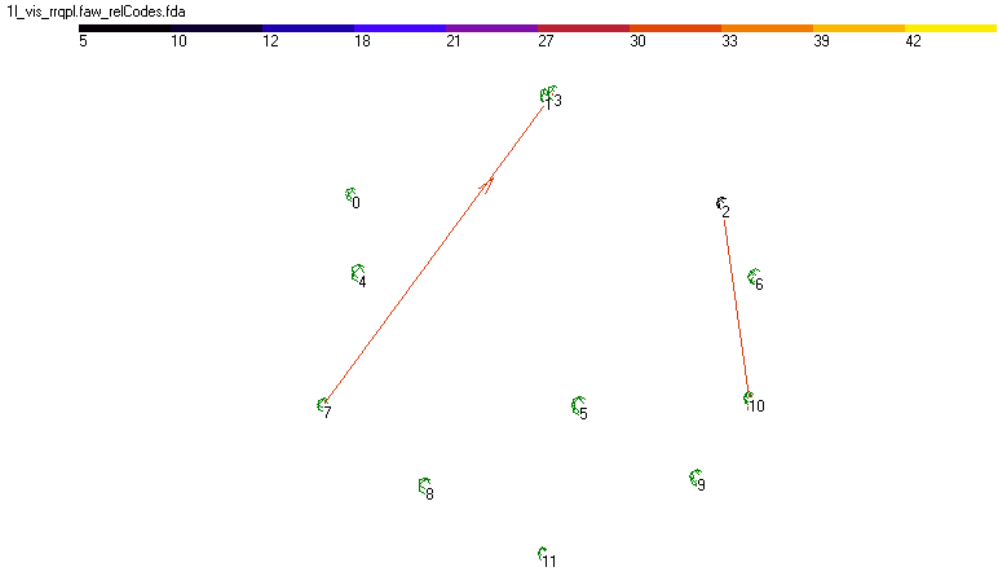

*C. Rhyme prepared – rhyme non-prepared, rhyme = left*

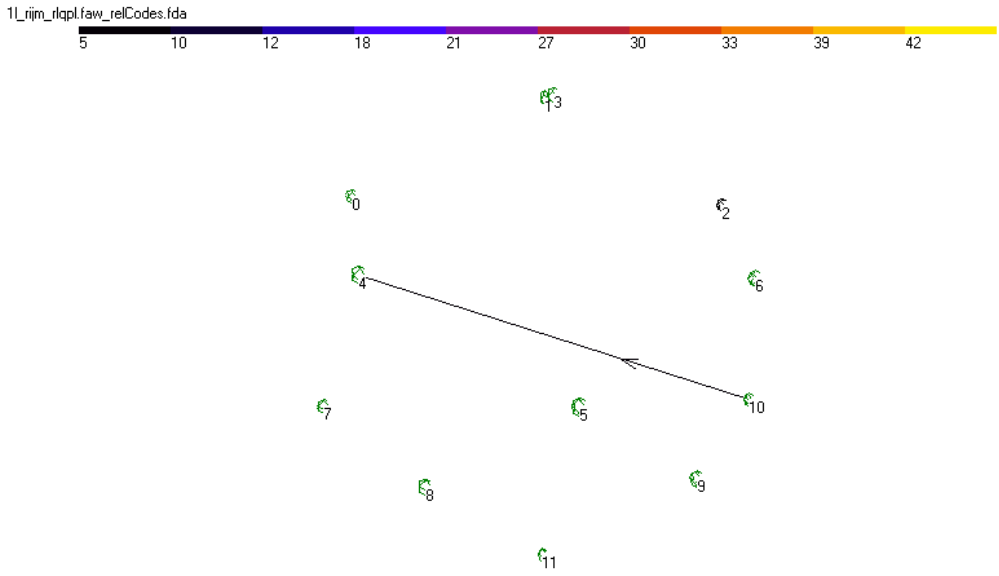


*D. Rhyme prepared – rhyme non-prepared, rhyme = right*

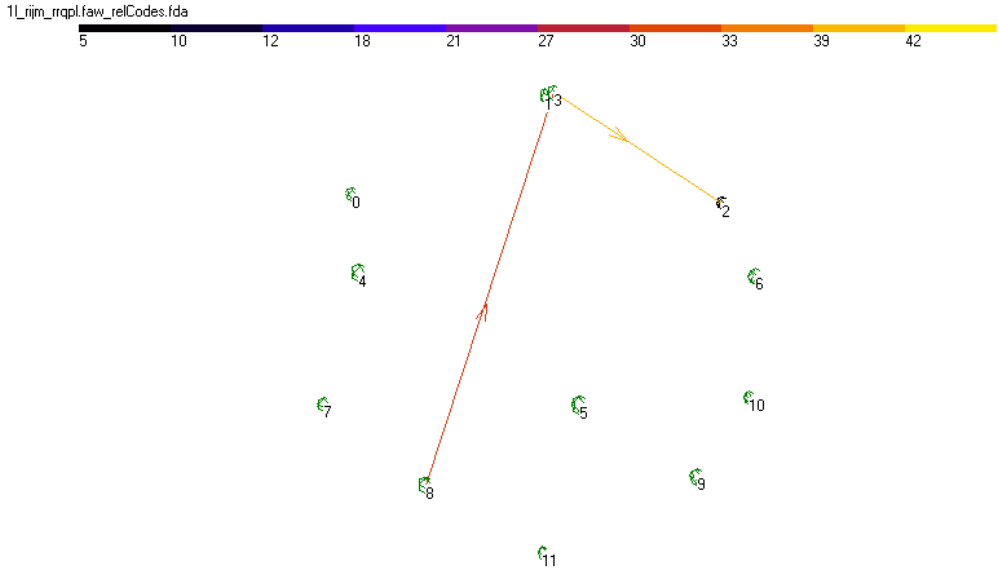

*Figure 3.12. EFA results: desynchronization*

*A. Visual prepared – visual non-prepared, rhyme = left*

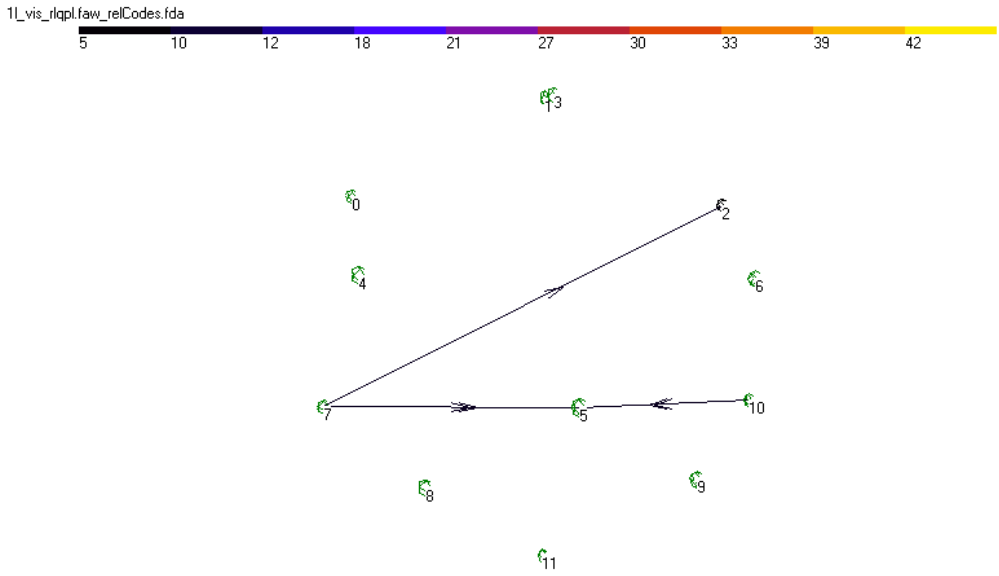


*B. Visual prepared – visual non-prepared, rhyme = right*

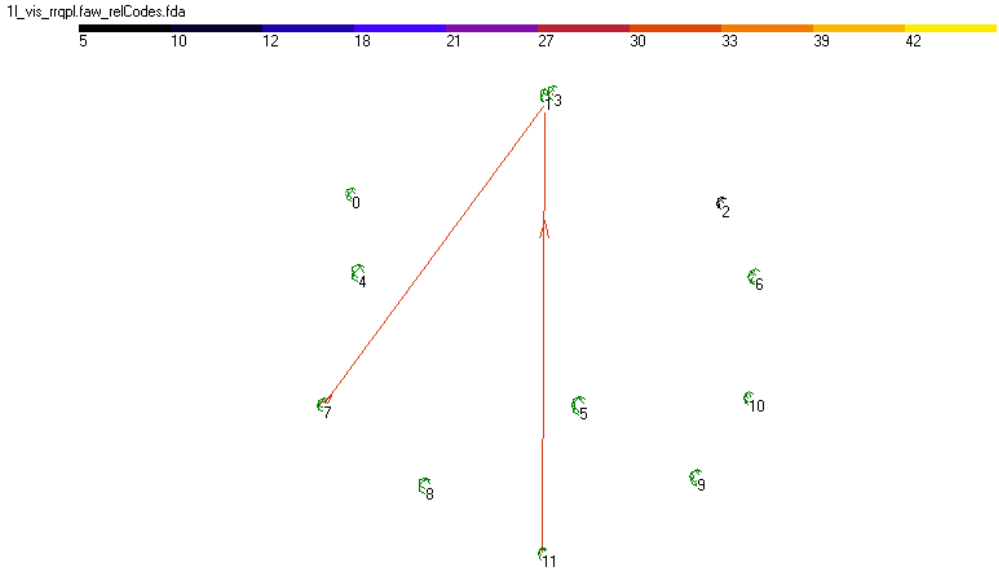

*C. Rhyme prepared – rhyme non-prepared, rhyme = left*

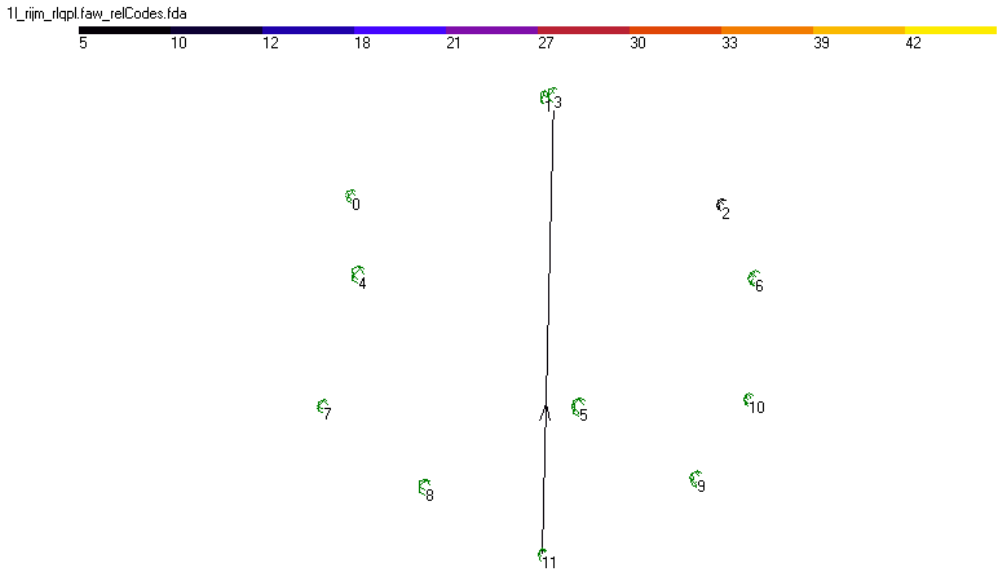


*D. Rhyme prepared – rhyme non-prepared, rhyme = right*

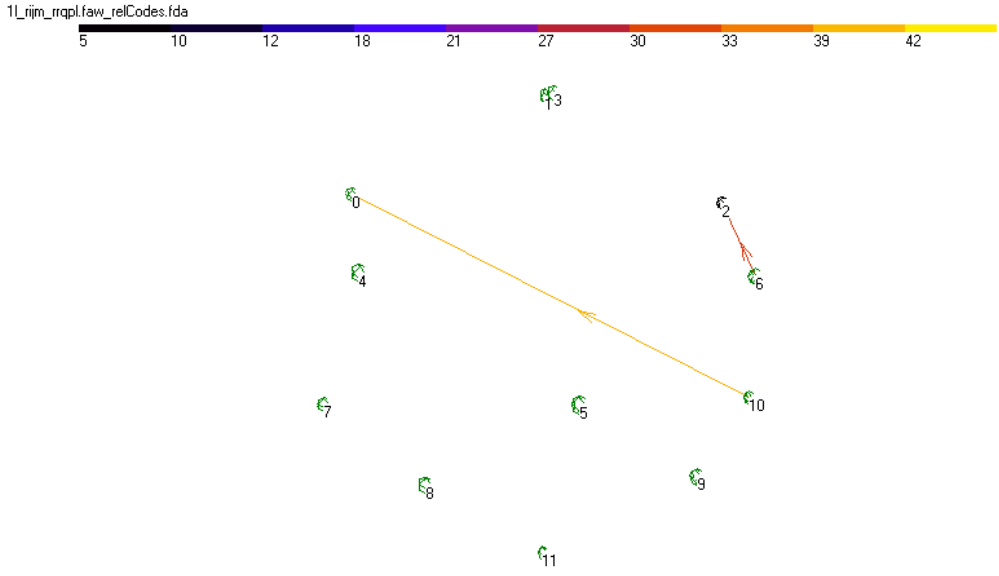


### 4.6. Discussion of the results

As far as they can be taken seriously, the data seem promising. First, the trends in the phase-locking measures supported the idea that synchrony plays a part in the anterior-posterior transient connections suggested in the introduction. Second, conspicuous effects on various measures were found which could be related to each other and interpreted together in a meaningful way. Recall that the pseudo-statistical QPL

results indicated different preparation styles for the two tasks. Preparation for the visual task seems to involve selection for action whereas preparation for the rhyme task is reflected by a process that may prevent the completion of local processes over irrelevant motor cortex. Together with the selectively visual LRP effect and the alpha burst in both conditions, the data seem to converge on the possibility that subjects prepare more actively for the visual task, which they must release or suppress as a kind of negative preparation for the rhyme task. It is uncertain whether this convergence will replicate, but it illustrates the way the various measures can provide an integrated view of underlying processes.

The prepared – non-prepared contrast, as mentioned above, is a complex measure because the non-prepared condition is not neutral. Differences may be caused either by switching processes in the prepared condition or oscillation and synchronies due to a residual task-set. The results presented here should, for proper data, be complemented by the results for the prepared and non-prepared conditions separately.

# 5. Discussion

It seems that wavelet analysis has the potential to be a valuable tool in the analysis of EEG signals. A domain of coding that the brain evidently uses is made available to analysis without violating the assumption of stationarity, or being forced to use relatively inelegant methods to work around such a violation whilst still using techniques which fundamentally depend on it. Results are embedded in a set of related psychophysiological models (cell assemblies, working with memory, the local / global theory) and anatomical / physiological theories and data (e.g. the corticothalamic pacemaker), which could enhance both the interpretability of results and their integration over experiments, researchers and disciplines.

Nevertheless, wavelet analyses are no better than the tools used to extract relevant information from their results. During our internship we were made aware of the way statistics are involved with every aspect of experimentation. This goes beyond the critical issues of replicability and statistical power. Because hypotheses are formulated using statistical concepts, the theories we can test come from a mental space delimited by our ability to determine meaningful stochastics. For instance, especially during the development of EFA (as we were more involved with working out the details of that method than principal spline analysis (PSA)) we felt as if we were using a more powerful approach than when we were simply using off-the-peg techniques such as repeated measures analysis into which our data "fitted". Our experience was no doubt partly based on maths deprivation due to different emphases laid in the path of our education. Nevertheless, deciding on what and how we would test in the detail necessary for implementation not only made vagueness impossible but also led us to think about the data and our own assumptions in new, more abstract ways. The EFA stochastics, unlike, for instance, repeated measurements performed on curves over time, make explicit the zero-sum (win - lose) situation between connections, perhaps a game played by fickle grandmothers (section 1.1.4), suggested by the theoretical function of specificity. This suggests that the application of game theory to the study of synchrony in the brain might prove insightful, whether or not EFA itself turns out to be a successful method.

A necessary improvement to the analysis train concerns the choice of ROI' s. During the present study, ROI' s were chosen based on rough approximations of the location of globally defined areas of the brain. One improvement would be to formulate hypotheses concerned only with certain electrodes, perhaps based on results from imaging methods with better spatial resolution. This approach has the advantages of specificity and data reduction. However, it may overlook important synchronies, and provides little or no information on specificity - finding synchrony between electrodes A an B may simply be the consequence of a global increase in synchrony. An alternative approach is data-driven selection such as in the following preliminary proposal. Following a CSD analysis, the data indicate proximity to a current source or sink. Current sources could then be estimated by adding sources at locations and with densities such that the explained current density variance is maximized, until the additional explained variance falls below a specified percentage, perhaps that which would be explained given a random current density distribution. The electrodes closest to the sources would then be selected for further analysis. Whilst we feel that such data-driven approaches provide an open-minded approach that may maximize statistical power, more work is required to determine their suitability.

In conclusion, the hypotheses described in this paper and its appendix remain to be properly tested. However, we have been able to formulate more specific hypotheses, and provide a priori interpretations of possible findings concerning oscillatory and synchronous activity. Most of the necessary methodology has been implemented, with the exception of the more powerful post-hoc EFA procedure and a measure for global changes in coherence, which seems especially interesting in the alpha band. Application of PSA to curves based on the sum of PLV / QPL (and perhaps the classical coherence measure) over ROI-pairs would provide a nonparametric method for the testing of differences in the time course of global coherence, with a number of tests equal to the number of frequencies. Given reasonable results concerning short-term visual memory, perceptual binding and preparation / selection in task-switching, wavelet analysis could be used to systematically work on a comprehensive theory of the role of synchrony in working with memory and the memory that is worked with. An important question such a theory should answer is how instructions lead to synchronies that result in the correct selection for action - if synchrony does indeed play that part.

# 6. References


Allison, T., Wood, C. C., and McCarthy, G. M. (1986). The central nervous system. In M. G. H. Coles, E. Donchin, and S. W. Porges (Eds.), *Psychophysiology systems, processes and applications*, 5-25. Guilford, New York.

Allport, D. A., Styles, E. A., and Hseih, S. (1994). Shifting attentional set: Exploring the dynamic control of tasks. In C. Umiltà and M. Moscovitch (Eds.), *Attention and Performance XV*, 421-452. Cambridge, MA: MIT Press.

Anderson, J.R., and Lebiere, C. (1998). *The Atomic Component of Thought* Erlbaum, Mahwah, New Jersey.

Azouz, R., and Gray, C. M. (2000). Dynamic spike threshold reveals a mechanism for synaptic coincidence detection in cortical neurons in vivo. *Proc. Natl. Acad. Sci. U.S.A.*, 10.1073/pnas.130200797v1.

Berger, H. (1929). Über das Elektrenkephalogramm des Menschen. *Archiv der Psychiatrie und Nervenkrankheit*, 87, 527–570.

Bertrand, O., Tallon-Baudry, C., Giard, M. H., and Pernier, J. (1998). Auditory induced 40-Hz activity during a frequency discrimination task. *NeuroImage*, 7, s370.

Bloomfield, P. (1976). *Fourier Analysis of Time Series: an Introduction*. John Wiley & Sons, New York.

Buhl, E. H., Tamás, G., and Fisahn, A. (1998). Cholinergic activation and tonic excitation induce persistent gamma oscillations in mouse somatosensory cortex in vitro. *Journal of Phsiology*, 513(1), 117-126.

Burgess, P. W., Veitch, E., de Lacy Costello, A., and Shallice, T. (2000). The cognitive and neuroanatomical correlates of multitasking. *Neuropsychologia*, 38, 848-863.

Cohen, J. D., Perlstein, W. M., Braver, T. S. & Nystrom, L. E. (1997). Temporal dynamics of brain activation during a working memory task. *Nature (London)*, 386, 604-608.

Corbetta, M., Kincade, J. M., Ollinger, J. M., McAvoy, M. P. & Schulman, G. L. (2000). Voluntary orienting is dissociated from target detection in human posterior parietal cortex. *Nat. Neuroscience*, 3, 292-297.

Courtney, S. M., Petit, L., Maisog, J. M., Ungerleider, L. G. & Haxby, J. V. (1998). An Area Specialized for Spatial Working Memory in Human Frontal Cortex. *Science*, 279, 1347-1351.

Damasio, A. R., and Damasio, H. (1994).Cortical systems for retrieval of concrete knowledge: The convergence zone framework. In Koch and Davis (Eds.), *Larg-scale neuronal theories of the brain*, 61-74. Cambridge, MA: MIT Press.

De Jong, R. (2000). An intention-activation account of residual switch costs. In S. Monsell and J. Driver (Eds.), *Attention and Performance XVIII: Cognitive control*. Cambridge: MIT Press.

Dove, A., Pollman, S., Schubert, T., Wiggins, C.J., and Cramon, D.Y. von. (1999). Prefrontal cortex activation in task switching: an event-related fMRI study. *Cognitive Brain Research*, 9(1), 103-109.

Eckhorn, R. (2000). Cortical processing by fast synchronization: high frequency rhythmic and non-rhythmic signals in the visual cortex point to general principles of spatiotemporal coding. In R. Miller (Ed.), *Time and the brain*, Harwood academic publishers.

Engel, A. K., König, P., and Singer, W. (1991). Direct physiological evidence for scene segmentation by temporal coding. *Proc. Natl. Acad. Sci. U.S.A.*, 88, 9136-9140.

Franowicz, M. N., and Barth, D. S. (1995), Comparison of evoked potentials and high-frequency (gamma-band) oscillating potentials in rat auditory cortex. *Journal of Neurophysiology,* 74, 96-112.

Fuster, J. M. (1997). Overview of prefrontal functions: The temporal organization of behavior. In J. M. Fuster (Ed.), *The prefrontal cortex*, 209-252. Lippincott-Raven.

Glaser, E. M., Ruchkin, D. S. (1976). *Principles of neurobiological signal analysis*. New York: Academic Press.

Gray, C. M., and McCormick, D A. (1996). Chattering cells: superficial pyramidal neurons contributing to the generation of synchronous oscillations in the visual cortex. *Science*, 274(5284), 109-113.

Haig, A.R., Gordon, E., Wright, J.J., Meares, R.A., Bahramali, H. (2000). Synchronous cortical gamma-band activity in task-relevant cognition. *NeuroReport,* 11(4), 669-675.

Harmony, T., Fernández, T., Silva, J., Bernal, J., Díaz-Comas, L., Reyes, A., Marosi, E., Rodríquez, M., and Rodríquez, M. (1996). EEG delta activity: an indicator of attention to internal processing during performance of mental tasks. *International Journal of Psychophysiology*, 24, 161-171.

Jersild, A. T. (1927). Mental set shift. *Archives of Psychology*, 9, whole issue.

Katznelson, R. D. (1981). Normal modes of the brain: Neuroanatomic basis and a physiologic theoretical model. In P. L. Nunez. (Ed.), *Electric fields of the brain: The neurophysics of EEG*, Oxford University Press.

Kimberg, D.Y., Aguirre, G.K., and D'Esposito, M. (2000). Modulation of task-related neural activity in task-switching: an fMRI study. *Cognitive Brain Research*, 10, 189-196.

Klimesch, W., Schimke, H., Doppelmayr, M., Ripper, B., Schwaiger, J., Pfurtscheller, G. (1996). Event-related desynchronization (ERD) and the Dm effect: Does alpha desynchronization during encoding predict later recall performance? *International Journal of Psychophysiology*, 24, 47-60.

Konish, S., Nakajima, K., Uchida, I., Kaneyama, M., Nakahara, K., Sekihara, K. & Miyahsita, Y. (1998). Transient activation of inferior prefrontal cortex during cognitive set shifting. *Nat. Neuroscience*, 1, 80-84.

Kopell, N., Ermentrout, G. B., Whittington, M. A. and Traub, R. D. Gamma rhythms and beta rhythms have different synchronization properties. *PNAS*, 97 (4), 1867 – 1872.

Kristeva-Feige, R., Feige, B., Makeig, S., Ross, B., and Elbert, T. (1993). Oscillatory brain activity during human sensorimotor integration. *NeuroReport*, 4, 1291-1294.

Lachaux, J. P., Rodriguez, E., Martinirie, J., and Varela, F. J. (1999). Measuring phase synchrony in brain signals. *Human Brain Mapping*, 8, 194-208.

Lorist, M. M., Klein, M., Nieuwenhuis, S., de Jong, R., Mulder, G. & Meijman, T. F. (2000). Mental fatigue and task control: Planning and preparation. *Psychophysiology*, 37 (5), 614-625.

Lutzenberger, W., Pulvermüller, F., and Birbaumer, N. (1994). Words and pseudowords elicit distinct patterns of 30-Hz activity in humans. *Neuroscince Letters,* 176, 115-118.

Lutzenburger, W. Pulvermüller, F., Elbert, T. Birbaumer, N. (1995). Local 40-Hz activity in human cortex induced by visual stimulation. *Neuroscience Letters*, 183, 39-42.

MacDonald, A. W., III, Cohen, J. D., Stenger, V. A. & Carter, C. S. (2000). Dissociating the Role of the Dorsolateral Prefrontal and Anterior Cingulate Cortex in Cognitive Control. *Science*, 288, 1835-1838.

Madler, C., and Pöppel, E. (1987). Auditory evoked potentials indicate the loss of neuronal oscillations during general anaesthesia. *Naturwissenschaften*, 74, 42-43.

Mendel, M.I.m and Goldstein, R. (1971). Early components of the averaged electroencephalographic response to constant-level clicks during all-night sleep. *Journal of Speech and Hearing Research*, 14, 829-840.

Moscovitch, M. (1992). Memory and working with memory: A component process model based on modules and central systems. *Journal of Cognitive Neuroscience*, 4, 257-267.

Murthy, V. N., and Fetz, E. E. (1992). Coherent 25 to 35 Hz oscillations in the sensorimotor cortex of awake behaving monkeys. *Proceedings of the National Academy of Sciences USA*, 89, 5670-74.

Norman, D. A., and Shallice, T. (1986). Attention to action: Willed and automatic control of behaviour. In R. Davison, G. Shwartz, and D. Shapiro (Eds.), *Consciousness and self regulation: Advances in research and theory*. New York: Plenum.

Nunez, P.L. (1981). *Electric fields of the brain: the neurophysics of EEG*. Oxford University Press, London.

Nunez, P. L. (1995). *Neocortical dynamics and human EEG rhythms.* Oxford University Press, London.

Nunez, P. L. (2000). Toward a quantitative description of large-scale neocortical dynamic function and EEG. *Behavioral and Brain sciences*, 23, 371-437.

Perrin, F., Pernier, J., Bertrand, O. and Echallier, J. F. (1989). Spherical splines for scalp potential and current density mapping. *Electroencephalography and Clinical Neurophysiology*, 72, 184 – 187. Correction in *Electroencephalography and Clinical Neurophysiology*, 76, 565.

Pfurtscheller, G., Flotzinger, D., and Neuper, C. (1994). Differentation between finger, toe and tongue movement in man based on 40 Hz EEG. *Electroencephalography and Clinical Neurophysiology,* 90, 456-460/

Pfurtscheller, G., Neuper, C., Pichler-Zalaudek, K., Edlinger, G., Lopes da Silva, F. (2000). Do brain oscillations of different frequencies indicate interaction between cortical areas in humans? *Neuroscience Letters*, 286, 66 – 68.

Posner, M. I. and Peterson, S. E. (1990). The attentional system of the human brain. *Annual Review of Neuroscience*, 13, 25 – 42.

Pulvermüller, F., Preissl, H., Lutzenberger, W., and Birbaumer, N. (1995). Spectral responses in the gamma-band: physiological signs of higher cognitive processes? *NeuroReport*, 6, 2057-2064.

Pulvermüller, F., Preissl, H., Lutzenberger, W., and Birbaumer, N. (1996). Brain rhythms of language: nouns versus verbs. *European Journal of Neuroscience*, 8, 937-941.

Pulvermüller, F. (1999). Words in the brain's language. *Behavioral and Brain sciences*, 22(2), 253-279.

Raz, J., Dickerson, L., and Turetsky, B. (1999). A wavelet packet model of evoked petentials. *Brain and Language*, 66, 61-88.

Roelfsema, P. R., Engel, A. K., and Singer, W. (1996). The role of neuronal synchronization in response selection: A biologically plausible theory of structured representations in the visual cortex. *Journal of Cognitive Neuroscience*, 8(6), 603-625.

Roelfsema, P. R., Engel, A. K., König, P. and Singer, W. (1997). Visuomotor integration is associated with zero time-lag synchronization among cortical areas. *Nature*, 385 (9), 157 – 161.

Rogers, R. D., and Monsell, S. (1995). Costs of a predictable switch between simple cognitive tasks. *Journal of Experimental Psychology: General*, 124, 207-231.

Samar, V.J., Bopardikar, A., Rao, R., Swartz, K. (1999). Wavelet analysis of neuroelectric waveforms: A conceptual tutorial. *Brain and Language*, 66(1), 7-60.

Sarnthein, J., Petsche, H., Rappelsberger, P., Shaw, G. L. and von Stein, A. (1998). Synchronization between prefrontal and posterior association cortex during human working memory. *Proceedings of the National Academy of Sciences USA*, 95, 7092-96.

Simon, H.A. (1994). The bottleneck of attention: Connecting thought with motivation. In D. Spaulding (Ed.), *Integrative views on motivation, cognition, and emotion: The Nebraska Symposium on Motivation,* 41, 1-21. Lincoln, NE: University of Nebraska Press.

Singer, W. (1990). Time as Coding Space. *Current Opinion in Neurobiology*, 9:189 – 194.

Singer, W. (1993) Synchronization of cortical activity and its putative role in information processing and learning. *Annual Reviews of Physiology*, 55, 349– 374.

Snijders, T. (2001). Principale splines bij herhaalde metingen. Personal communication.

Sohn, M. H., Ursu, S., Anderson, J.R., Stenger, V.A., and Carter, C.S. (2000). The role of prefrontal cortex and posterior parietal cortex in task switching. *Proceedings*

*of the National Academy of Sciences of the United States of America*, 97(24), 13448-13453.

Spydell, J. D., and Sheer, D. E. (1982). Effect of problem solving on right and left hemisphere 40 hertz EEG activity. *Psychophysiology*, 19, 420-425.

Sukov, W., and Barth, D. S. (2001). Cellular mechanisms of thalamically evoked gamma oscillations in auditory cortex. *Journal of Neurophysiology*, 85(3), 1235-1245.

Tallon-Baudry, C., Bertrand, O., Bouchet, P., and Pernier, J. (1995). Gamma-range activity evoked by coherent visual stimuli in humans. *European Journal of Neuroscience*, 16, 4240-4249.

Tallon-Baudry, C., Bertrand, O., Peronnet, F., and Pernier, J. (1998). Induced gamma-band activity during the delay of a visual short-term memory task in humans. *Journal of Neuroscience*, 18(11), 4244-4254.

Tallon-Baudry, C., and Bertrand, O. (1999). Oscillatory gamma activity in humans and its role in object representation. *Trends in cognitive sciences*, 3(4), 151-162.

Tipper, S.P., and Driver, J. (1988). Negative priming between pictures and words: Evidence for semantic analysis of ignored stimuli. *Memory and Cognition*, 16, 64-70.

Traub, R. D., Jefferys, J. R., and Whittington, M. A. (1999). *Fast oscillations in cortical circuits.* Cambridge, MA: MIT Press.

Vogel, W., Broverman, D.M., and Klaiber, E.L. (1968). EEG and mental abilities. *Electroencephalography and Clinical Neurophysiology,* 24, 166-175.

Yantis, S., Meyer, D.E., and Smith, J.E.K. (1991). Analyses of multinomial mixture distributions: New tests for stochastic models of cognition and action. *Psychological Bulletin*, 110, 350-374.

# 7. Appendix A. Pilot tasks

## 7.1. Introduction

One of our two pilot tasks was a replication of an experiment by Tallon-Baudry and Bertrand (1998). The other was an elaboration of their design based on theory and evidence presented in section 1.1. Our data were unusable due to malfunctions and it would be worthwhile to acquire new data for these tasks. The designs are less complex than the task-switching paradigm and would have been, and still would be, good starting points for exploring rhythmic responses to stimuli in well-known psycho(-physio-)logical paradigms.

## 7.2. Replication: matching task

In this task, two wobbly-circle stimuli around a fixation cross were presented with a separating delay. The matching task was to remember the first stimulus and determine whether the second was identical. In the control task, subjects had only to detect infrequent dimmings of the fixation cross. In the original study, a burst of 30 Hz activity was found during the delay of the matching task, that was absent during the control task. In our replication we also looked at phase-locking between groups of electrodes. Tallon-Baudry (1998) provide further details of the design, including the polar equation used to calculate the wobbly circles (mathematically, Lagrange polynomials).

The reason for using wobbly circles was that we expected specific forms to be hard to store verbally, making an iconic strategy more likely. The most important hypothesized synchronies were thus between putative working-with-memory (Moscovitch, 1992; Burgess, 2000) areas and visual cortex, most importantly the prefrontal - occipital connection. The control task was intended to provide visual attention without rehearsal in working memory. However, the stimulus to be detected in the control condition is presented after a known delay. Subjects didn't actually have to pay attention during the delay, only towards the end before the dimming might occur. Perhaps using a variable delay would make the control condition a stronger test. The control task was also reported by subjects to be intensely boring; some even

mentioned strange visual effects like shifting walls and a kind of tunnel vision. A lot of breaks, more than the four we used, seem to be necessary.

### 7.3. Extension: property binding

A visual scene containing two wobbly circles is built up of two positions and two shapes. We expect synchrony to be likely to transiently connect the positions and shapes within each of the two forms, and to separate them from each other. Occipital and posterior temporal areas are known to represent object information, whereas location is represented in parietal cortex (e.g. Posner & Peterson, 1990). Therefore, we expect a pattern of synchrony to occur involving these three areas when a complex stimulus consisting of two Lagrange polynomials must be retained during a delay.

Our design to test this was similar to the matching experiment described above. However, instead of a matching and a control condition we used three different kinds of matching conditions. Matching forms, locations and both form and location of the stimuli were the matching criteria. To test for the effect of task-difficulty we included a more difficult version of the form-matching condition in which the wobbly circles had less pronounced characteristics. When only forms or only locations had to be retained, we expected synchrony between anterior (especially prefrontal) and occipital / posterior temporal and parietal areas respectively. When both forms and locations were to be matched, we expected to find synchrony between the object-related and location-related areas, and anterior regions.